

# Optimal Mass Transport and Its Applications in Computer Vision, Medical Imaging and Visualization

Zhengyu Su

Advisor: Prof. Xianfeng Gu

## **Committee members:**

Professor. Xianfeng Gu

Professor. Jie Gao

Professor. Jing Chen

# Overview

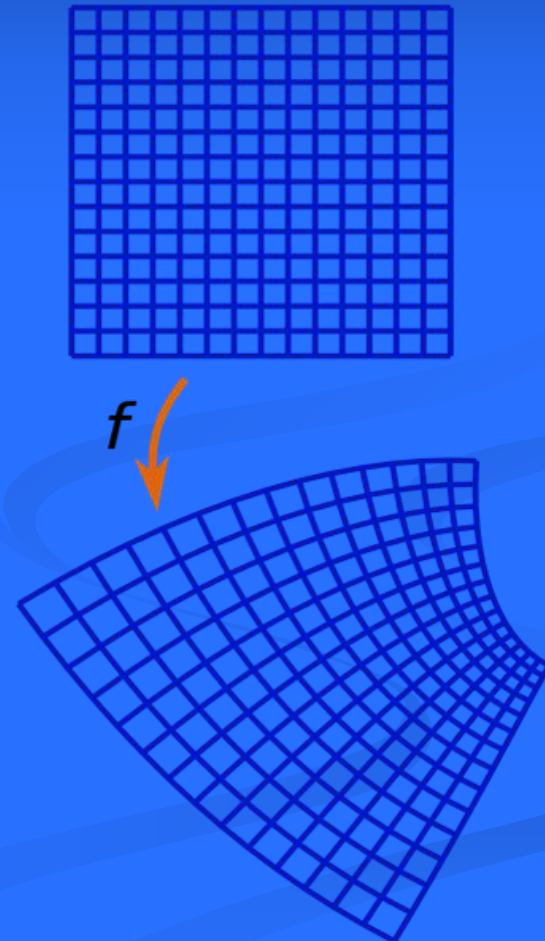
- Introduction
- Theoretical Background
- Algorithms
- Applications
  - Computer Vision
  - Medical Imaging
  - Visualization
- Conclusion

# Introduction

- 3D Surface representation and parameterization play fundamental roles in computer vision, medical imaging and visualization, etc.
- Conventional conformal mapping gives the limitations that it may introduce large area distortions and cause numerical problems.
- Optimal Mass Transport map serves as a more powerful tool in many applications.

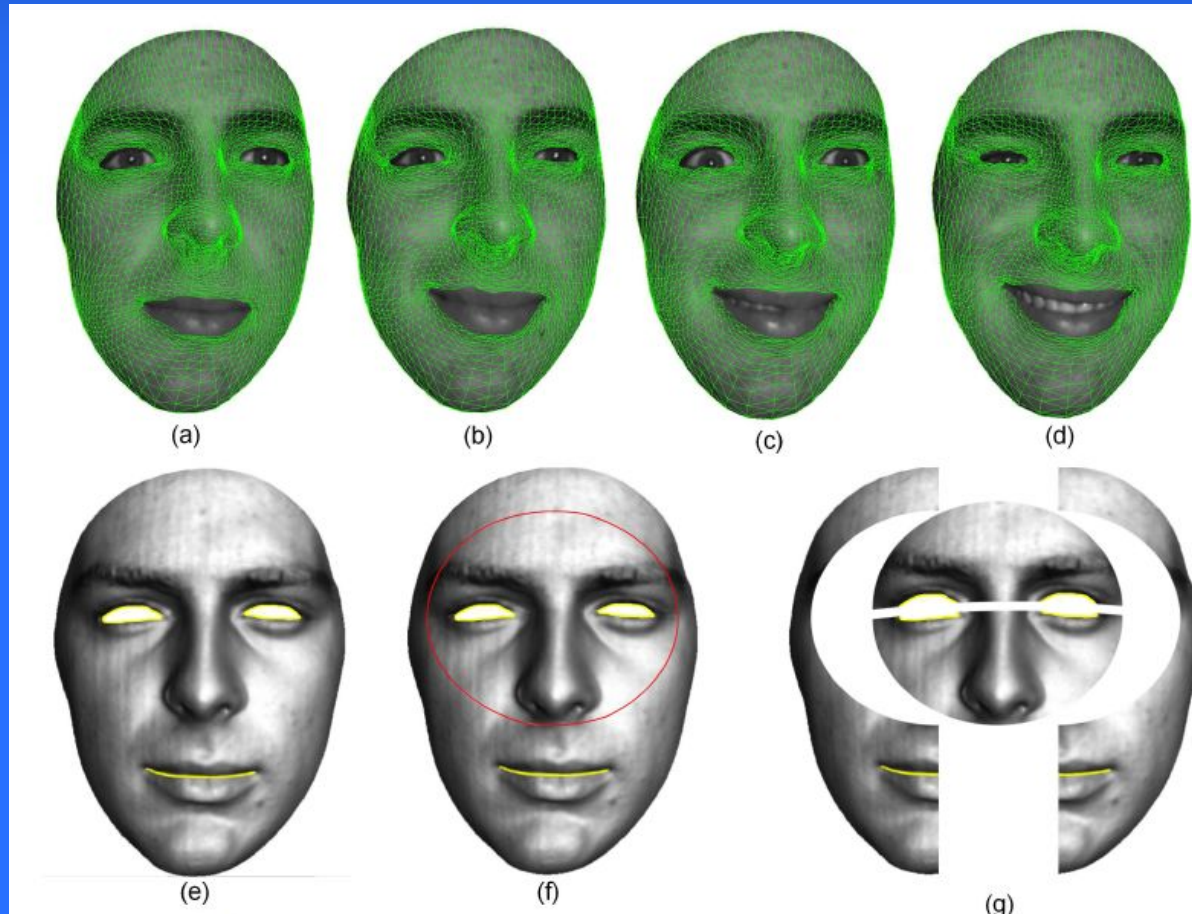
# Conventional Method

- A conformal map is a map  $f:U \rightarrow V$ , which preserves angles.



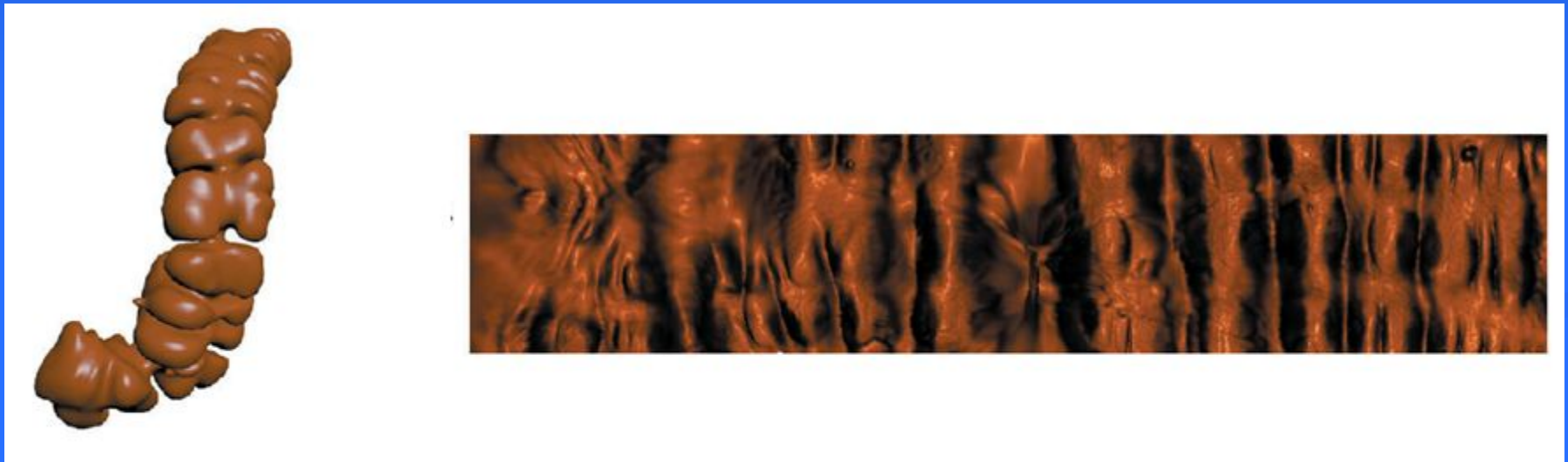
# Introduction

- Face tracking by hyperbolic harmonic map.



# Introduction

## ■ Virtual Colonoscopy

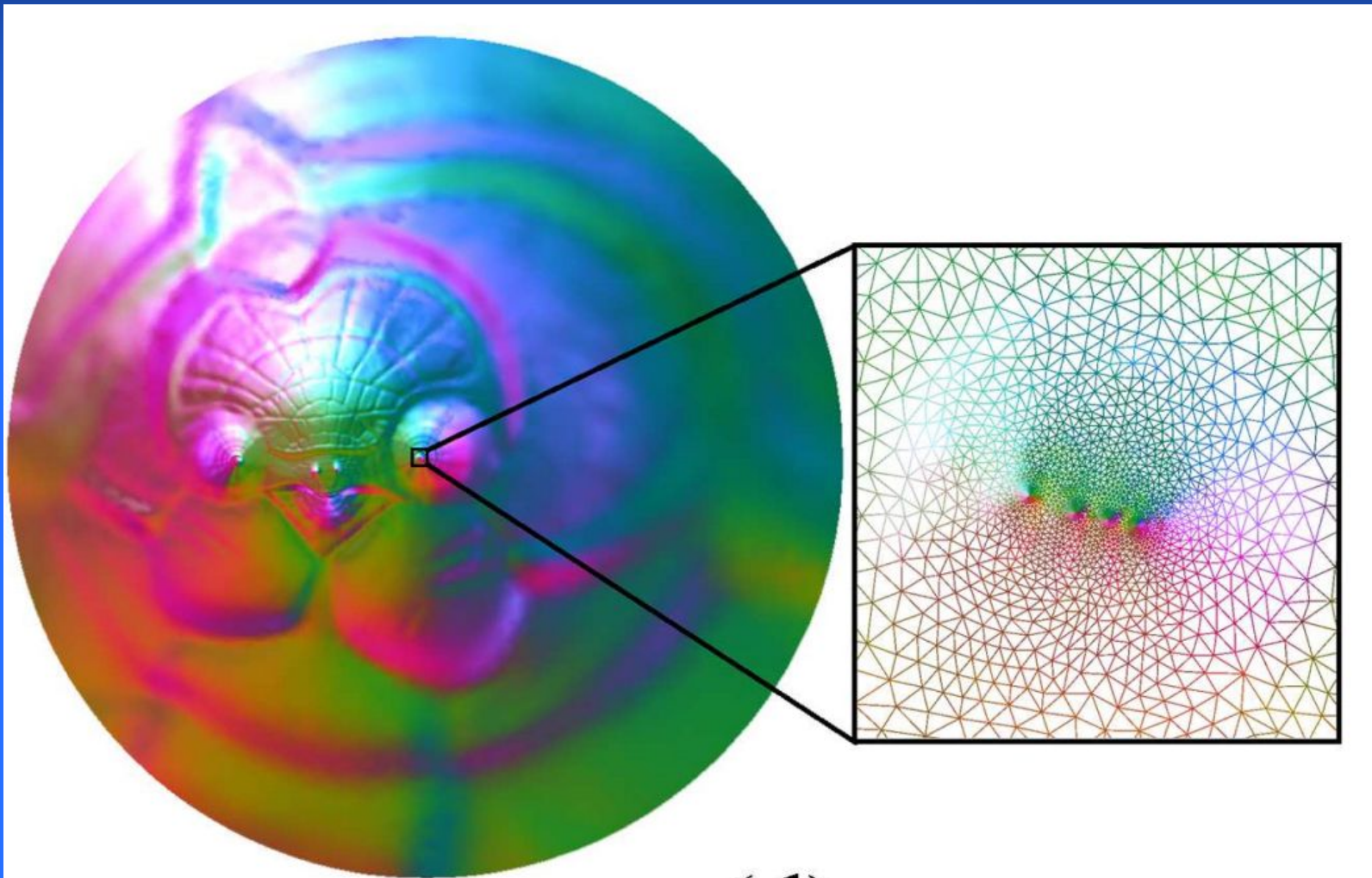


# Introduction

- Disadvantage of Conformal map:
  - It usually introduces large area distortions, and may even cause numerical problems especially for long tube cases.



# Introduction



(d)

# Introduction

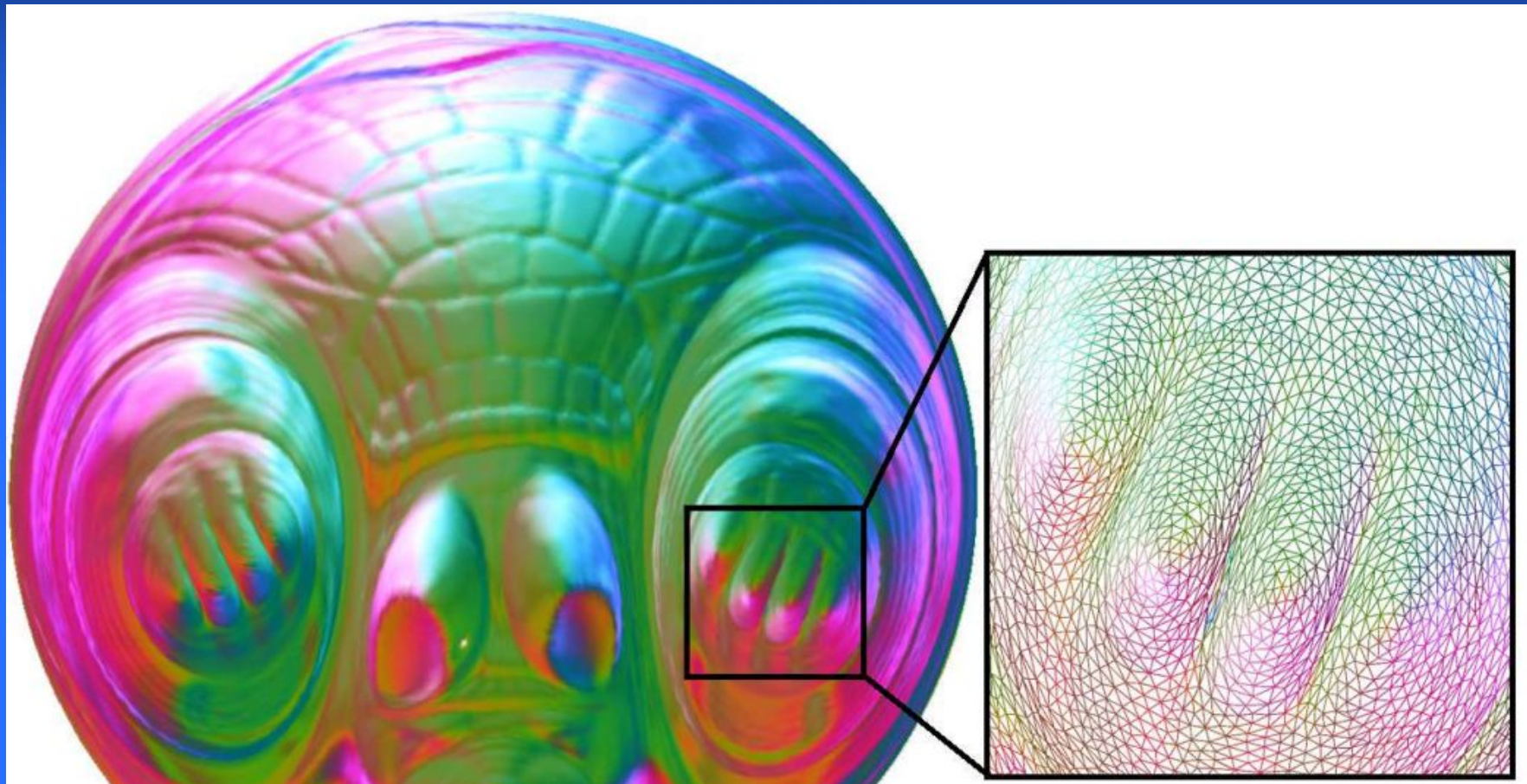
- Motivation:

A 3D surface mapping method which minimizes area distortions is highly desired.

- Solution:

Optimal Mass Transport Map

# Introduction



(c)

# Pioneering Work

- Allan Tannenbaum pioneered the optimal mass transport theory in medical imaging and computer vision field.
  - S. Haker, L. Zhu, A. Tannenbaum, and S. Angenent. Optimal mass transport for registration and warping. International Journal on Computer Vision, 60(3):225–240, 2004.
  - T. Rehman, E. Haber, G. Pryor, and A. Tannenbaum. Fast optimal mass transport for 2D image registration and morphing. Elsevier Journal of Image and Vision Computing, 2008.
  - T. Rehman, E. Haber, G. Pryor, J. Melonakos, and A. Tannenbaum. 3D nonrigid registration via optimal mass transport on the GPU. Medical Image Analysis, 13:931–40, 2009.
  - A. Dominitz and A. Tannenbaum. Texture mapping via optimal mass transport. IEEE Transactions on Visualization and Computer Graphics, 16(13):419–432, 2010.

# Pioneering Work

- Ni et. al applied the optimal mass transport theory for internet topology analysis.
  - Chien-Chun Ni, Yu-Yao Lin, Jie Gao, Xianfeng Gu, Emil Saucan, Ricci Curvature of the Internet Topology, Proceedings of the 34th Annual IEEE International Conference on Computer Communications (INFOCOM'15), April-May, 2015.
- Computer graphics work
  - Q. Merigot. A multiscale approach to optimal transport. Comput. Graph. Forum. 30(5):1583–1592, 2011.
  - F. de Goes, K. Breeden, V. Ostromoukhov, and M. Desbrun. Blue noise through optimal transport. ACM Trans. Graph. (SIGGRAPH Asia), 31:1–10, 2012.

# Introduction

## ■ Our approach:

- Based on Yau-Luo-Gu's variational principle [1].
  - [1] X. Gu, F. Luo, J. Sun, and S.-T. Yau. Variational principles for Minkowski type problems, discrete optimal transport, and discrete Monge-Amper  equations. arXiv:1302.5472, 2013.
- Extended from 2D domain to 3D surface.
- Complexity: reduces from  $O(n^2)$  to  $O(n)$  comparing to Monge-Kantorovich's approach.

# Introduction

## ■ Merits:

- Uniqueness: Due to the convexity of the energy, our method has a unique solution.
- Diffeomorphism: If the domains are convex, The optimal mapping is guaranteed to be diffeomorphic.
- Efficiency: Due to the convexity of the energy, it can be optimized using Newton's method.
- Simplicity: The computational algorithm is mainly based on (power) Voronoi diagram and Delaunay triangulation.
- Intrinsic: The map between two surfaces is solely determined by the surface Riemannian metric, therefore it is intrinsic.

# Theoretical Background

- Conformal Map
- Optimal Mass Transport Map

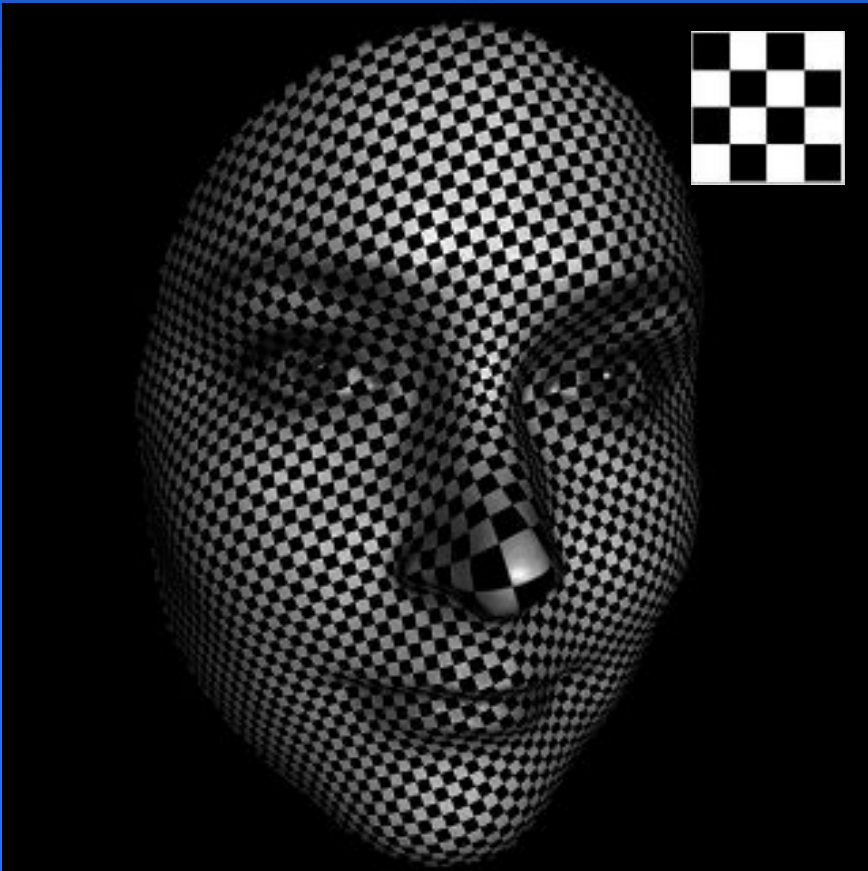
# Conformal Map

**Definition (Conformal Mapping)** Suppose  $(S_1, g_1)$  and  $(S_2, g_2)$  are two Riemannian surfaces, a mapping  $\varphi : S_1 \rightarrow S_2$  is conformal, if the pull back metric  $\varphi^*g_2$  induced by  $\varphi$  on  $S_2$  differs from the original metric  $g_1$  by a scalar

$$\varphi^*g_2 = e^{2\lambda}g_1,$$

where  $\lambda : S_1 \rightarrow \mathbb{R}$  is called a conformal factor.

# Conformal Map



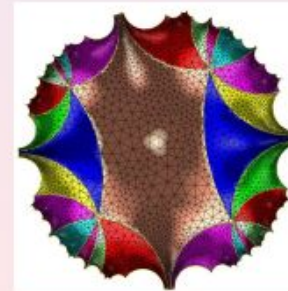
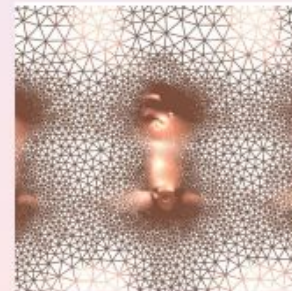
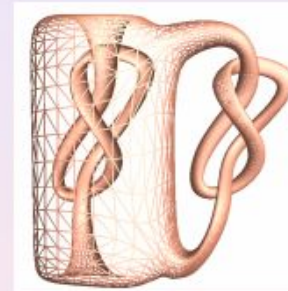
# Conformal Map

**Theorem (Uniformization)** Suppose  $(S, g)$  is a closed compact Riemannian surface with genus  $g$ , then there is a conformal factor function  $\lambda : S \rightarrow \mathbb{R}$ , such that the conformal metric  $e^{2\lambda}g$  induces constant Gaussian curvature. Depending on the genus is 0, 1 or greater than 1, the const is +1, 0 or -1.

# Conformal Map

## Theorem (Poincaré Uniformization Theorem)

Let  $(\Sigma, \mathbf{g})$  be a compact 2-dimensional Riemannian manifold. Then there is a metric  $\tilde{\mathbf{g}} = e^{2\lambda} \mathbf{g}$  conformal to  $\mathbf{g}$  which has constant Gauss curvature.



Spherical

Euclidean

Hyperbolic

# Conformal Map

- Uniformization Algorithm by Ricci Flow method
- Suppose the surface  $S$  has a Riemannian metric  $g$ , Gaussian curvature:

$$K(u, v) = -\Delta_g \lambda(u, v) = -\frac{1}{e^{2\lambda(u,v)}} \left( \frac{\partial^2}{\partial u^2} + \frac{\partial^2}{\partial v^2} \right) \lambda(u, v),$$

- The Ricci flow is defined as heat diffusion process:

$$\frac{d\mathbf{g}(t)}{dt} = 2(\bar{K}(t) - K(t)),$$

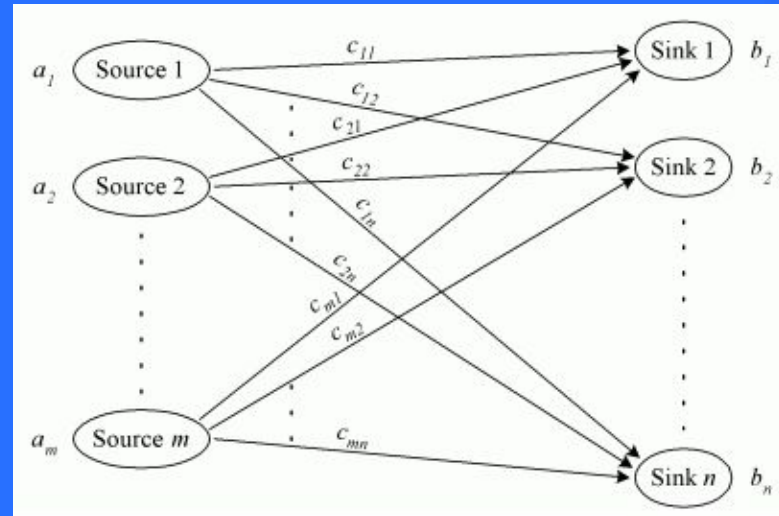
# Optimal Mass Transport Map

## ■ Optimal Mass Transport (OMT) Problem

- Classical OMT problem proposed in 1781 by Monge: with minimal transportation cost, to move a pile of soil from one place to another



French mathematician,  
father of differential  
geometry



Transportation cost for moving from  $s \in S$  to  $d \in D$  is  $c(s, d)$

# Optimal Mass Transport Map

## ■ Mathematical Definition

*Problem (Optimal Mass Transport):* Suppose  $(X, \mu)$ ,  $(Y, \nu)$  are metric space with probabilities measures, which have the same total mass  $\int_X \mu dx = \int_Y \nu dy$ . A map  $T : X \rightarrow Y$  is *measure preserving*, if for any measurable set  $B \subset Y$ ,  $\mu(T^{-1}(B)) = \nu(B)$ . Given a transportation cost function  $c : X \times Y \rightarrow \mathbb{R}$ , find the measure preserving map  $T : X \rightarrow Y$  that minimizes the total transportation cost

$$\mathcal{C}(T) := \int_X c(x, T(x)) d\mu(x).$$

# Optimal Mass Transport Map

## ■ Kantorovich's Approach

- In the 1940s, Leonid Kantorovich introduced the relaxation of Monge's problem and founded linear programming method.
- [L. V. Kantorovich. On a problem of Monge. *Journal of Mathematical Sciences*, 3:225–226, 1948.].
- Won the Nobel Prize in 1975

# Optimal Mass Transport Map

## ■ Kantorovich's Approach

Kantorovich constructed a measure  $\mu(x, y) : \Omega_0 \times \Omega_1 \rightarrow \mathbb{R}$ , which minimizes the cost

$$\int_{\Omega_0 \times \Omega_1} |x - y|^2 \mu(x, y) dx dy,$$

with the constraints

$$\int_{\Omega_1} \mu(x, y) dy = \mu_0(x), \int_{\Omega_0} \mu(x, y) dx = \mu_1(y).$$

- The method requires  $O(n^2)$  variables.

# Optimal Mass Transport Map

**Power Diagram** Consider a collection of points  $P = \{p_1, p_2, \dots, p_k\}$  in  $\mathbb{R}^n$ . Suppose each point  $p_i \in P$  has a power (weight)  $h_i \in \mathbb{R}$ . The *power distance* from a point  $x \in \mathbb{R}^n$  to  $p_i$  is defined as

$$\text{Pow}(x, p_i) = \frac{1}{2} \|x - p_i\|^2 - \frac{1}{2} h_i.$$

The *power diagram* of  $\{(p_i, h_i)\}$  is a partition of the  $\mathbb{R}^n$  into  $k$  cells  $W_i$ , such that a point  $x$  belongs to  $W_i$  whenever

$$Pow(x, p_i) = \min_j Pow(x, p_j).$$

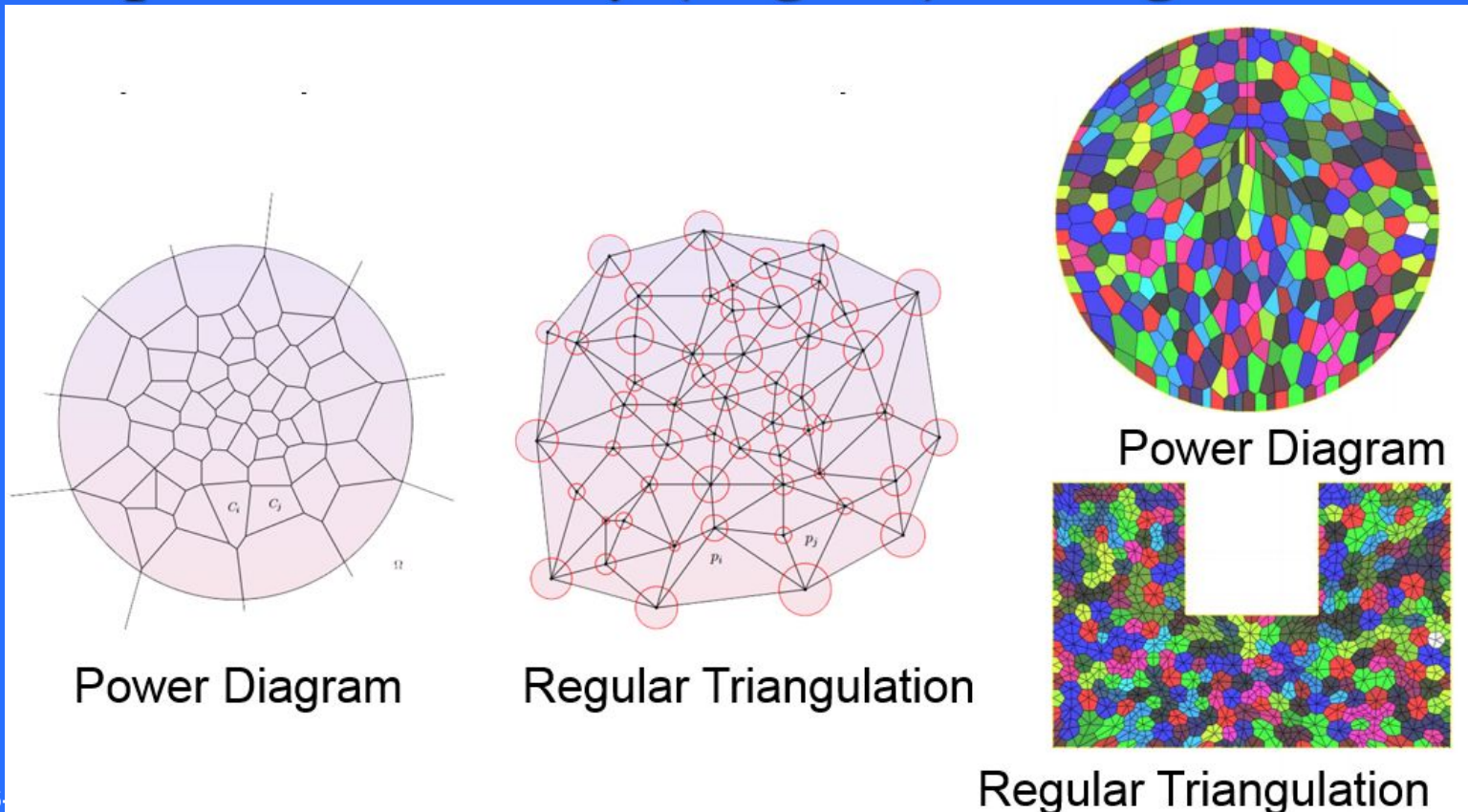
# Optimal Mass Transport Map

The power diagram partitions of the Euclidean plane into polygonal cells,  $\{W_i\}$

$$\begin{aligned} W_i &= \{x | Pow(x, p_i) \leq Pow(x, p_j), \forall j\} \\ &= \{x | \langle x, p_i \rangle + 1/2(h_i - |p_i|^2) \geq \langle x, p_j \rangle + 1/2(h_j - |p_j|^2), \forall j\} \end{aligned}$$

# Optimal Mass Transport Map

- The dual graph of the power diagram is called the power Delaunay (Regular) Triangulation



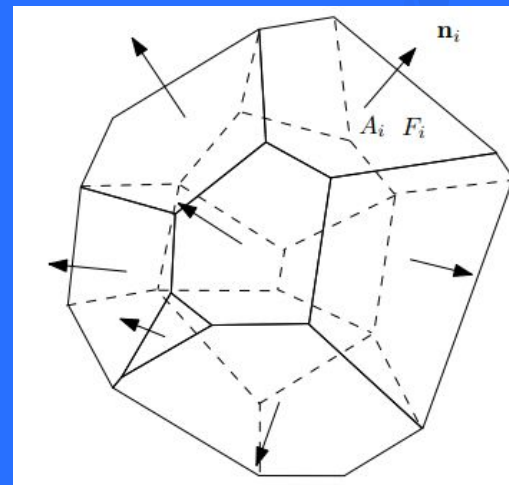
# Optimal Mass Transport Map

## ■ Minkowski theory

**Theorem 1 (Minkowski [5])** Given  $k$  unit vectors  $\mathbf{n}_1, \dots, \mathbf{n}_k$  not contained in a half-space in  $\mathbb{R}^n$  and  $A_1, \dots, A_k \geq 0$ , such that

$$\sum_{i=1}^k A_i \mathbf{n}_i = 0,$$

then there exists a convex polytope  $P$  with faces  $F_1, \dots, F_k$ , such that the normal to  $F_i$  is  $\mathbf{n}_i$  and the area of  $F_i$  is  $A_i$ .  $P$  is unique up to translations.



# Optimal Mass Transport Map

## ■ Alexandrov's generalization

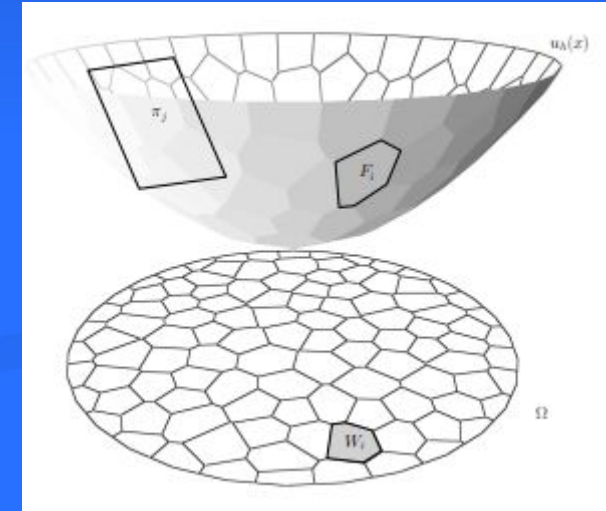
Alexandrov generalized Minkowski's result to non-compact convex polyhedra. As shown in Fig.2, given  $k$  planes  $\pi_i : \langle x, p_i \rangle + h_i$ , one can construct a piecewise linear convex function

$$u(x) = \max_i \{ \langle x, p_i \rangle + h_i | i = 1, \dots, k \}, \quad (1)$$

whose graph is an infinite convex polyhedron. The PL convex function produces a convex cell decomposition  $\{W_i\}$  of  $\mathbb{R}^n$ :

$$W_i = \{x | \langle x, p_i \rangle + h_i \geq \langle x, p_j \rangle + h_j, \forall j\} = \{x | \nabla u(x) = p_i\}. \quad (2)$$

Alexandrov shows that the convex polyhedron is determined by the face normal, or equivalently the gradient  $\{p_i\}$  and the projected area  $\{A_i\}$ .



- Recall that Eqn. 2 has the same form of the power decomposition.

$$\begin{aligned} W_i &= \{x | Pow(x, p_i) \leq Pow(x, p_j), \forall j\} \\ &= \{x | \langle x, p_i \rangle + 1/2(h_i - |p_i|^2) \geq \langle x, p_j \rangle + 1/2(h_j - |p_j|^2), \forall j\} \end{aligned}$$

# Optimal Mass Transport Map

## ■ Alexandrov theory

**Theorem 2 (Alexandrov [8])** Given a compact convex domain  $\Omega$  in  $\mathbb{R}^n$ , if  $p_1, \dots, p_k$  are distinct in  $\mathbb{R}^n$ ,  $A_1, \dots, A_k > 0$  such that

$$\sum_{i=1}^k A_i = \text{vol}(\Omega),$$

then there exists a piecewise linear function  $u(x) = \max_i \{\langle x, p_i \rangle + h_i\}$  unique up to translations, such that

$$\text{Vol}(W_i \cap \Omega) = A_i,$$

where  $W_i$  is defined in Eqn. 2.

**Definition 2 (Alexandrov map)** We call the gradient map  $\nabla u : x \rightarrow \nabla u(x)$  the Alexandrov map, or briefly A-Map.

# Optimal Mass Transport Map

## ■ Brenier's theory

According to Monge-Brenier theory [1], the Alexandrov map is the unique Optimal Mass Transport map, that minimizes the following mass transport energy

$$\int_{\Omega} \|x - f(x)\|^2 dx,$$

among all mass preserving maps  $f : \Omega \rightarrow \{p_1, \dots, p_k\}$ , such that

$$Vol(f^{-1}(p_i)) = A_i.$$

[1]Y. Brenier, Polar factorization and monotone rearrangement of vector-valued functions, Com. Pure Appl. Math., vol. 64, pp. 375-417, 1991.

# Optimal Mass Transport Map

## ■ Monge-Ampere equation

$$\begin{cases} \det(\text{Hess}(w))(x) = A(x, w(x), \nabla w(x)) \\ w|_{\partial\Omega} = g \end{cases}$$

- Shing-Tung Yau proved the existence and uniqueness of Monge-Ampere equation.
- Optimal mass transport problem is equivalent to solve the Monge-Ampere equation.

# Optimal Mass Transport Map

- Yau-Luo-Gu gives a constructive proof to Alexandrov map, based on variational principle
  - X. Gu, F. Luo, J. Sun, and S.-T. Yau. Variational principles for Minkowski type problems, discrete optimal transport, and discrete Monge-Amper  equations. arXiv:1302.5472, 2013.
- Our approach follows this variational principle. converts the optimal mass transport problem to a convex optimization problem and can be solved by Newton's method.
- Complexity:  $O(n)$

# Optimal Mass Transport Map

## ■ Our variational principle

**Theorem 3 (Generalized Alexandrov)** Given a convex domain  $\Omega \subset \mathbb{R}^n$ , with measure density  $\rho : \Omega \rightarrow \mathbb{R}$ , and a discrete point set  $P = \{p_1, \dots, p_k\}$  with discrete measures  $\mu = \{\mu_1, \dots, \mu_k\}$ , such that

$$\int_{\Omega} \rho(x) dx = \sum_{i=1}^k \mu_i,$$

then there exists a  $\mathbf{h} = \{h_1, \dots, h_k\}$  unique upto translations, such that the convex function  $u(x) = \max_i \{\langle x, p_i \rangle + h_i\}$ , induces a cell decomposition of  $\mathbb{R}^n$ ,  $\mathbb{R}^n = \bigcup_{i=1}^k W_i(\mathbf{h})$ , and the area of each cell

$$w_i(\mathbf{h}) = \int_{W_i(\mathbf{h}) \cap \Omega} \rho(x) dx$$

equals to  $\mu_i$ .  $\mathbf{h}$  is the unique global minimizer of the convex function

$$E_{\mu}(\mathbf{h}) = \sum_{i=1}^k \mu_i h_i - \int_{\mathbf{0}}^{\mathbf{h}} \omega,$$

where the differential form  $\omega = \sum_{i=1}^k w_i(\mathbf{h}) dh_i$ .

# Algorithm

## ■ Optimal Mass Transport Map Algorithm

■ Energy:

$$E_{\mu}(\mathbf{h}) = \sum_{i=1}^k \mu_i h_i - \int_{\mathbf{0}}^{\mathbf{h}} \omega, \quad (1)$$

■ Gradient:

$$\nabla E(\mathbf{h}) = (w_1(\mathbf{h}) - \nu_1, \dots, w_k(\mathbf{h}) - \nu_k)^T \quad (2)$$

■ Hessian:

$$\frac{\partial^2 E(\mathbf{h})}{\partial h_i \partial h_j} = \begin{cases} \frac{\int_{e_{ij}} \mu(x) dx}{|y_j - y_i|} & W_i(\mathbf{h}) \cap W_j(\mathbf{h}) \cap \Omega \neq \emptyset \\ 0 & otherwise \end{cases} \quad (3)$$

---

**Algorithm 1** Optimal Mass Transport Map (OMT-Map)

---

**Input:** A convex planar domain with measure  $(\Omega, \mu)$ ; a planar point set with measure  $(P, \nu)$ ,  $\nu_i > 0$ ,  $\int_{\Omega} u(x)dx = \sum_{i=1}^k \nu_i$ ; a threshold  $\epsilon$ .  
**Output:** The unique discrete OMT-Map  $f : (\Omega, \mu) \rightarrow (P, \nu)$ .

Scale and translate  $P$ , such that  $P \subset \Omega$ .

$\mathbf{h} \leftarrow (0, 0, \dots, 0)$ .

Compute the power diagram  $D(\mathbf{h})$ ,

Compute the dual power Delaunay triangulation  $T(\mathbf{h})$ ,

Compute the cell areas  $\mathbf{w}(\mathbf{h}) = (w_1(\mathbf{h}), \dots, w_k(\mathbf{h}))$ .

**repeat**

    Compute  $\nabla E(\mathbf{h})$  using Eqn. 2.

    Compute the Hessian matrix using Eqn. 3.

$\lambda \leftarrow 1$

$\mathbf{h} \leftarrow \mathbf{h} - \lambda H^{-1} \nabla E(\mathbf{h})$ .

    Compute  $D(\mathbf{h})$ ,  $T(\mathbf{h})$  and  $\mathbf{w}(\mathbf{h})$

**while**  $\exists w_i(\mathbf{h}) == 0$  **do**

$\mathbf{h} \leftarrow \mathbf{h} + \lambda H^{-1} \nabla E(\mathbf{h})$ .

$\lambda \leftarrow 1/2\lambda$

$\mathbf{h} \leftarrow \mathbf{h} - \lambda H^{-1} \nabla E(\mathbf{h})$ .

        Compute  $D(\mathbf{h})$ ,  $T(\mathbf{h})$  and  $\mathbf{w}(\mathbf{h})$ .

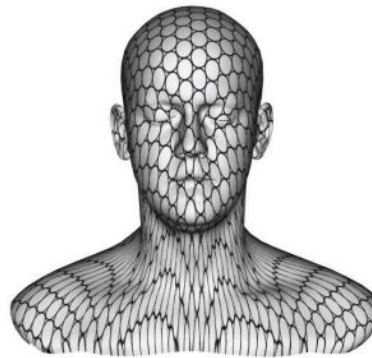
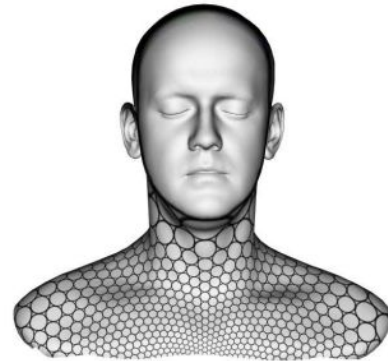
**end while**

**until**  $\|\nabla E\| < \epsilon$ .

**return**  $f : \Omega \rightarrow P$ ,  $W_i(\mathbf{h}) \rightarrow p_i, i = 1, 2, \dots, k$ .

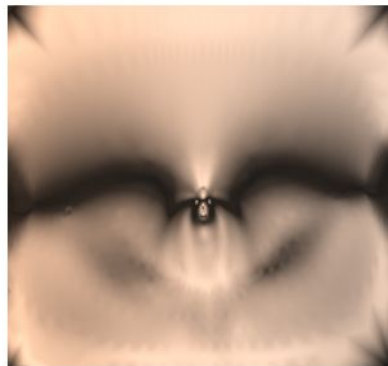
---

# Algorithm



(a) texture mapping by CFP

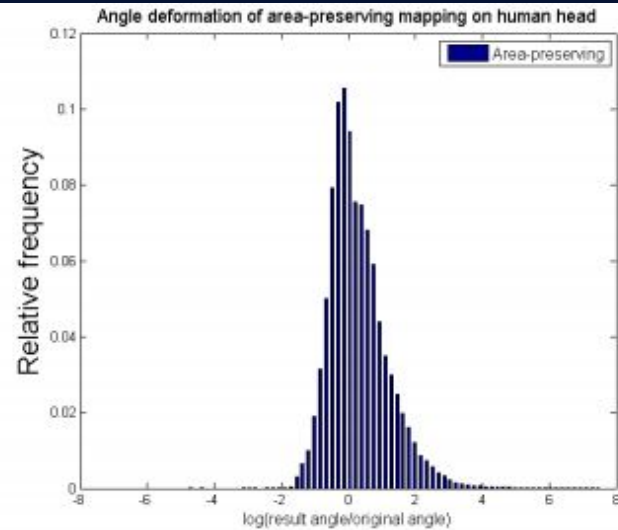
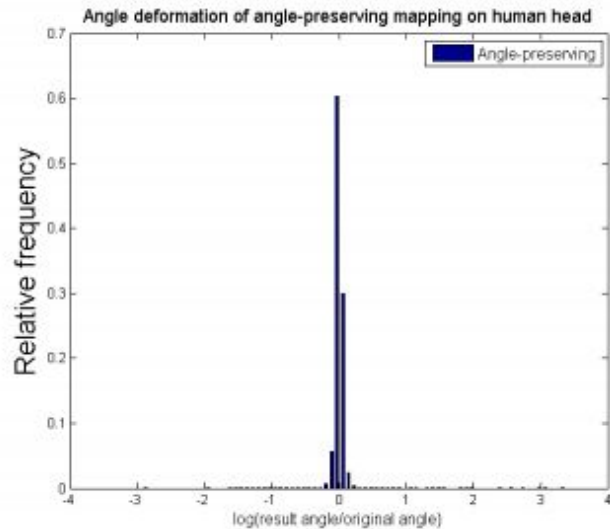
(b) texture mapping by APP



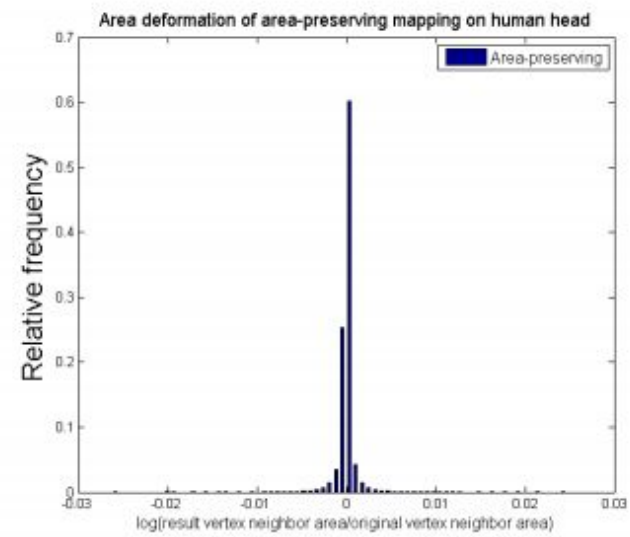
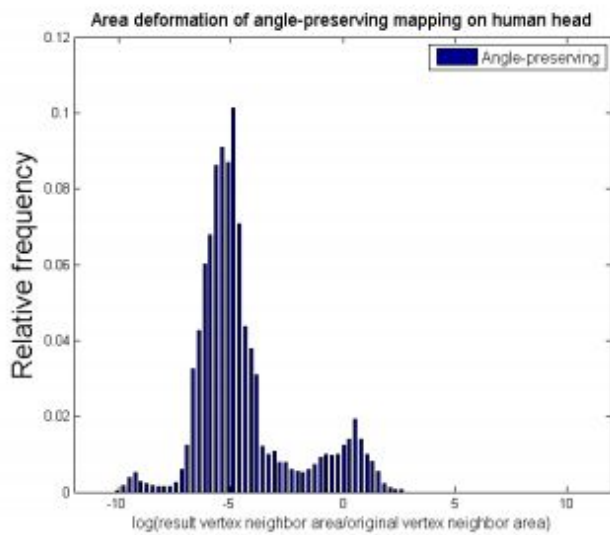
(c) angle-preserving



(d) area-preserving



(e) angle distortion by CFP (f) angle distortion by APP



(g) area distortion by CFP (h) area distortion by APP



(a) front view



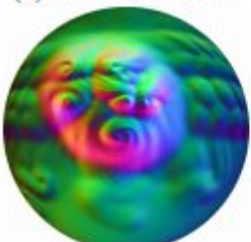
(b) back view



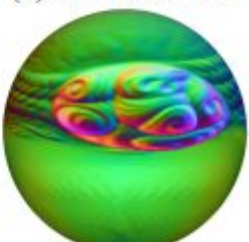
(c) CFP front view



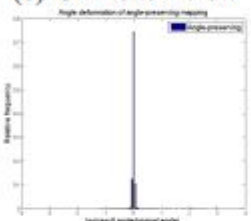
(d) APP front view



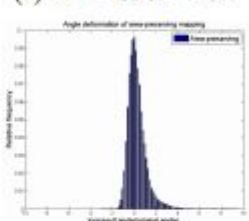
(e) CFP back view



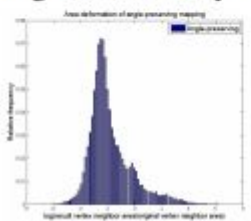
(f) APP back view



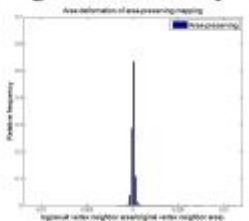
(g) angle distortion by CFP



(h) angle distortion by APP



(i) area distortion by CFP



(j) area distortion by APP

# Applications

- **Computer Vision**—Optimal Mass Transport for Shape Analysis
- **Medical Imaging**—Area Preserving Brain Mapping
- **Visualization**—Optimal Mass Transport for Scientific Visualization

# Optimal Mass Transport for Shape Analysis

## ■ Motivation:

- With fast development of 3D scanning technologies, surface based shape representation is of great importance for 3D computer vision.
- A rigorous and efficient surface based approach would be highly advantageous in this research field.

# Optimal Mass Transport for Shape Analysis

- Propose to use optimal mass transport map for shape matching and comparison, focusing on two important applications.
  - Surface registration.
  - 3D Shape classification.

# Optimal Mass Transport for surface registration

- Surface registration:
  - Find the 1-to-1 and onto correspondences between the surfaces.
  - It provides many advantages for down-streaming applications such as medical diagnosis.

# Optimal Mass Transport for surface registration

- Difficulty:
  - Studying the original 3D surfaces could be extremely difficult when shapes are irregular and complex, such as human brain cortical surfaces.

# Optimal Mass Transport for surface registration

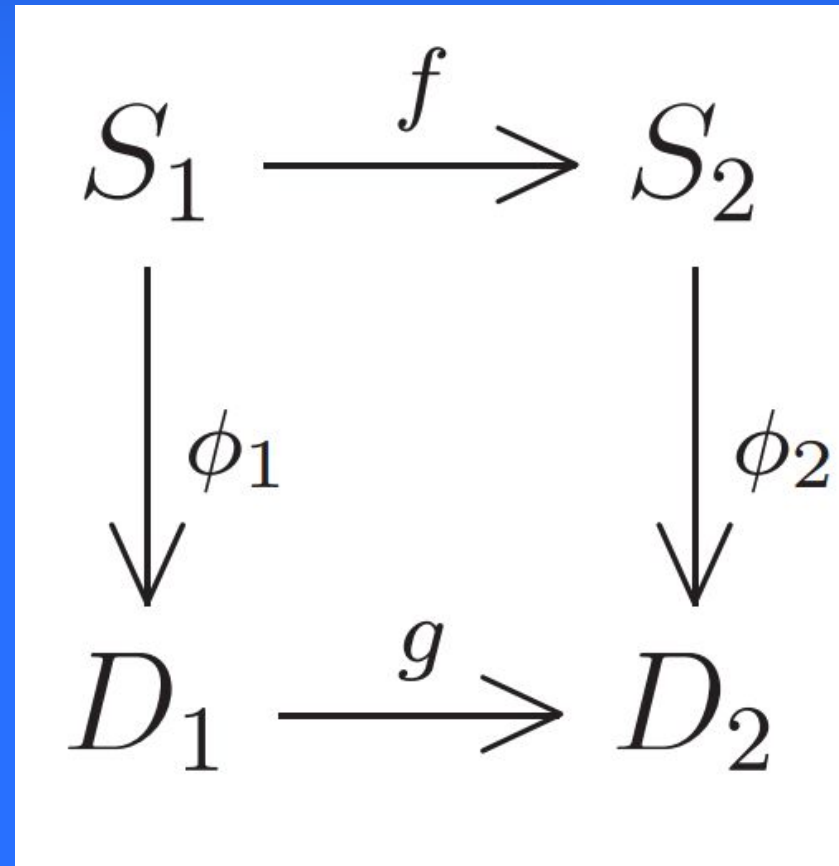
- One effective and common approach is to first parameterize the original 3D domain to some classical parameter domains, such as planar or spherical domain, then register 3D surfaces through these canonical space
- Conventional conformal map based methods:
  - Minimizes angle distortions.
  - But introduces large area distortions and may even cause numerical problems.

# Optimal Mass Transport for surface registration

- Our solution:
  - Build a robust and efficient surface registration pipeline by optimal mass transport map would be highly desired.

# Pipeline

- Register between S1 and S2



# Algorithm Pipeline

---

**Algorithm 4** Deformable surface registration.

---

**Input:** Triangular meshes of surfaces with a simple topology, such as a simply connected domain with one boundary. A template surface as the target surface.

**Output:** Registered surfaces with a one-to-one correspondence from each surface to the target surface.

1. Manually or automatically locate some corresponding feature points on  $S_1$  and  $S_2$  for constraints.
  2. Compute a constrained harmonic map  $g : D_1 \rightarrow D_2$ , such that  $g$  align the corresponding feature points specified in the first step.
  3. The matching is given by  $f = \phi_2^{-1} \circ g \circ \phi_1 : S_1 \rightarrow S_2$ .
-

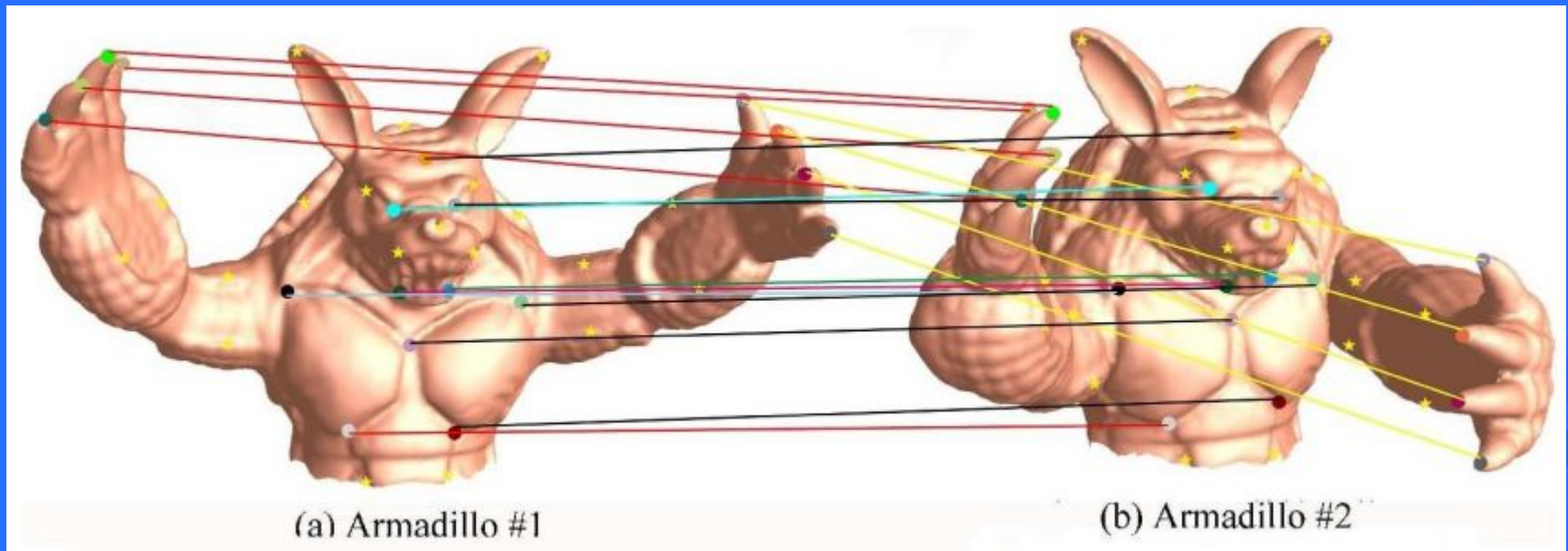
# Experimental Results

- We chose 7 models that are isometric deformations to each other to study the accuracy and efficiency.



# Experimental Results

- Their mapping results are matched using harmonic maps with hard constraints (yellow stars). The colored lines connecting color-encoded circular dots on (a) and (b) show the registered correspondences by OMT map.



# Experimental Results

## ■ Evaluation and comparison

- We compared our method with conformal map based registration method [1], and Möbius voting method [2].
- [1] [Y. Wang, J. Shi, X. Yin, X. Gu, T. F. Chan, S. T. Yau, A. W. Toga, and P. M. Thompson. Brain surface conformal parameterization with the Ricci flow. IEEE TMI, 31(2):251–264, 2012.]
- [2] [Y. Lipman and T. Funkhouser. Möbius voting for surface correspondence. TOG, 28(3), Aug 2009].

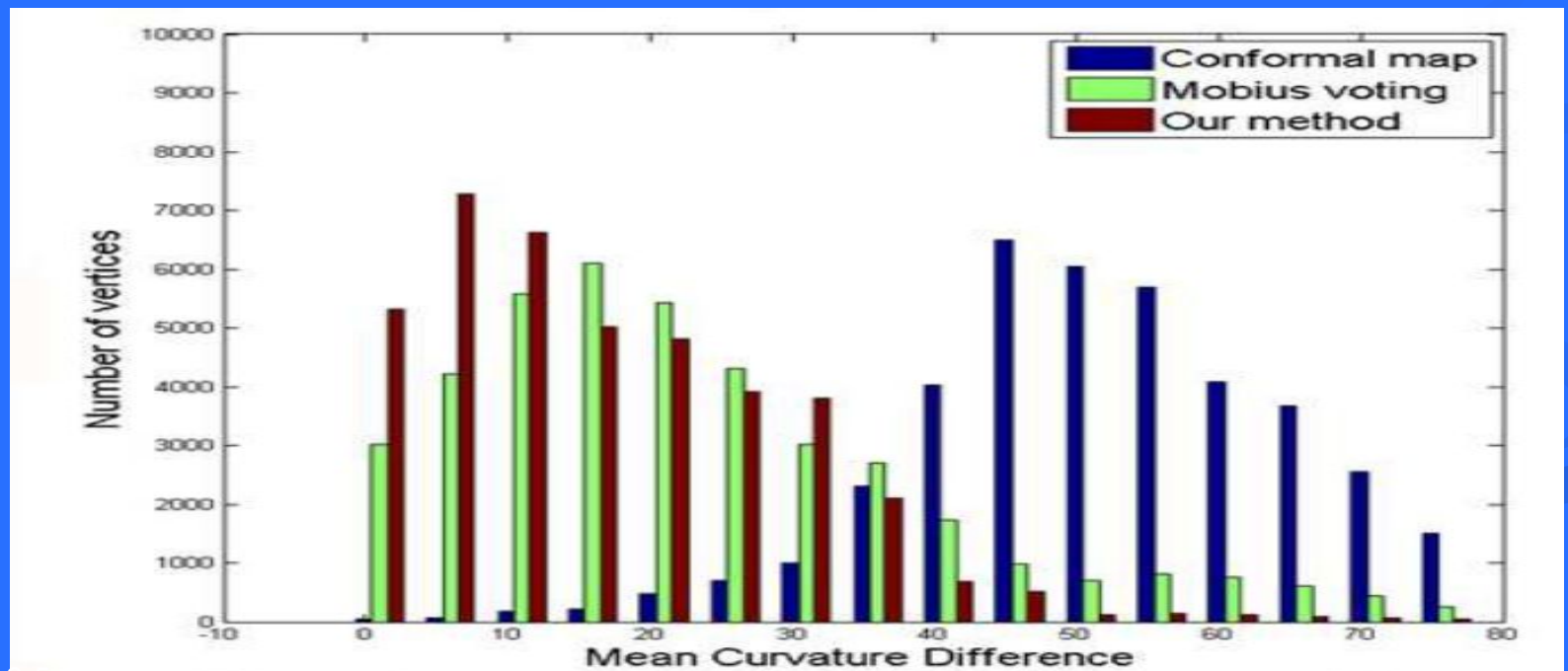
# Experimental Results

- Evaluation and comparison
  - Diffeomorphism: For each registration, we compute the Jacobian determinant and measure the area of flipped regions.

	average flipped area
Conformal map	25.8%
Mobius voting	4.5%
Our method	0%

# Experimental Results

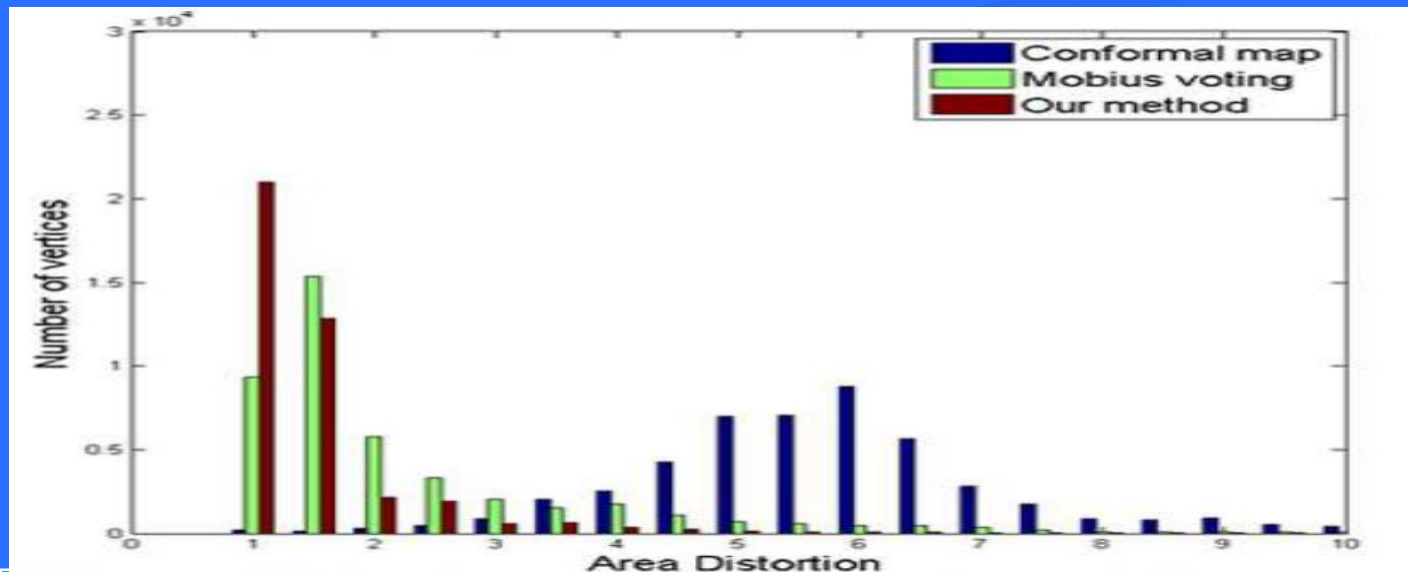
- Evaluation and comparison
  - Curvature Difference Map: We quantified the effects of registration on curvature by computing the difference of curvature maps from the registered surfaces.



# Experimental Results

## ■ Evaluation and comparison

- Local Area Distortion: For each vertex  $v$  on the target surface with its correspondent point  $p$  on the source surface, we compute its Jacobian determinant  $J(v)$ , and represent the local area distortion at  $v$  as  $\max(J(v), 1/J(v))$ .



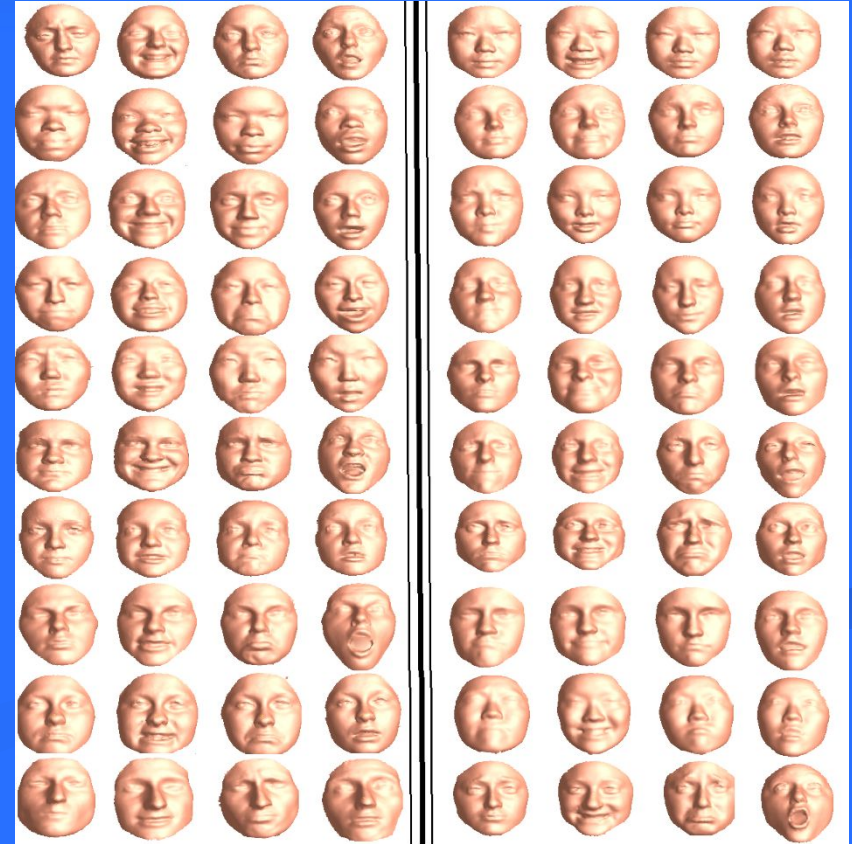
# 3D Shape Classification

## ■ Motivation:

- 3D shape classification is a fundamental problem in computer vision.
  - 3D shape searching
  - 3D object recognition.

## ■ Difficulties:

- High dimensions.
- Boundary parameterization.



# 3D Shape Classification

## ■ Existing works review:

- Topology based method [1], computes 3D shape similarity by comparing Multi-resolution Reeb Graphs, yet they can not describe the geometric differences.
- Statistical based method [2], represents objects with feature vectors in a multidimensional space, but they are not discriminating enough to make subtle distinctions between shapes.

[1] M. Hilaga, Y. Shinagawa, T. Kohmura, and T. Kunii. Topology matching for fully automatic similarity estimation of 3d shapes. SIGGRAPH 2001, 21:203–212, 2001

[2] R. Osada, T. Funkhouser, B. Chazelle, and D. Dobkin. Shape distributions. Symposium  
2016-5<sup>25</sup> Large Spatial Databases, 21:807–832, 2002

# 3D Shape Classification

- Our solution:
  - Conformal Wasserstein distance to measure the shape dissimilarities.
- Why?
  - Based on conformal mapping and optimal mass transport map.
  - Gives a Riemannian metric for the Wasserstein space.
  - Intrinsically measures the dissimilarities between shapes.

# Theoretic foundation

## ■ Wasserstein shape space:

Suppose  $(M, g)$  is a Riemannian manifold with a Riemannian metric  $g$ .

*Definition (Wasserstein Space):* Let  $\mathcal{P}_p(M)$  denote the space of all probability measures  $\mu$  on  $M$  with finite  $p^{th}$  moment, where  $p \geq 1$ . Suppose there exists some point  $x_0 \in M$  that  $\int_M d(x, x_0)^p d\mu(x) < +\infty$ , where  $d$  is the geodesic distance induced by  $g$ .

# Theoretic foundation

## ■ Wasserstein distance:

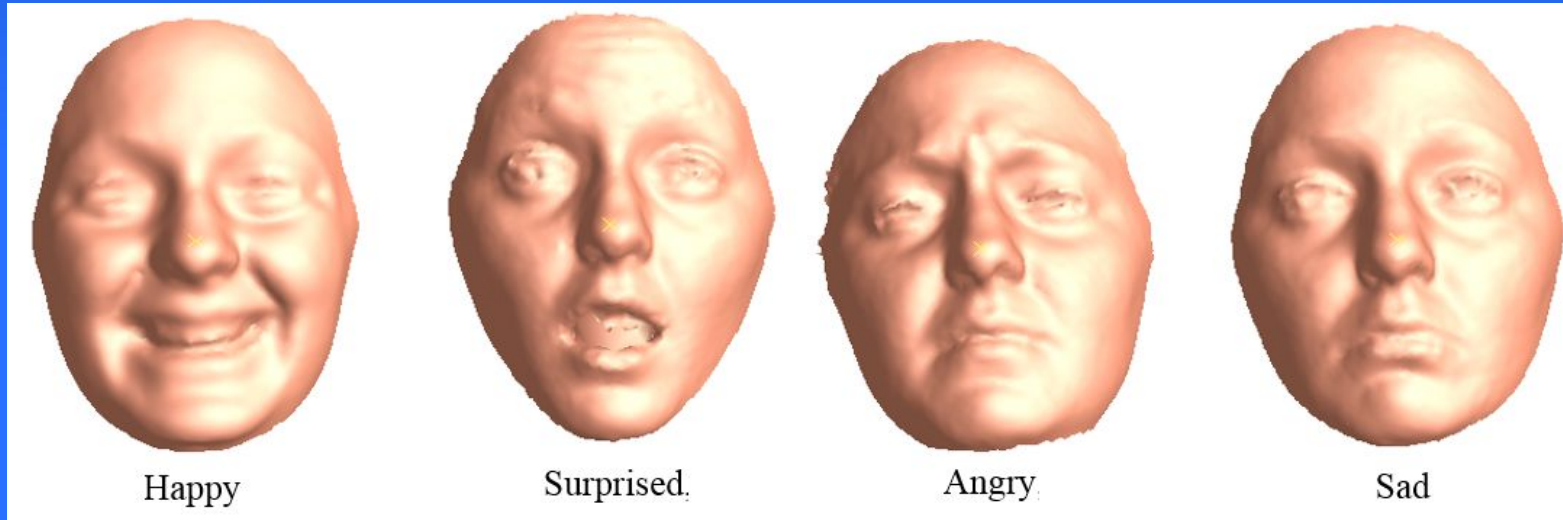
Given two probability  $\mu$  and  $\nu$  in  $\mathcal{P}_p$ , the Wasserstein distance between them is defined as the transportation cost induced by the optimal mass transport map  $T : M \rightarrow M$ ,

$$W_p(\mu, \nu) := \inf_{T_\# \mu = \nu} \left( \int_M d(x, T(x))^p d\mu(x) \right)^{\frac{1}{p}}.$$

## ■ Our optimal mass transport map algorithm gives a practical way of computing Wasserstein distance.

# Experimental results

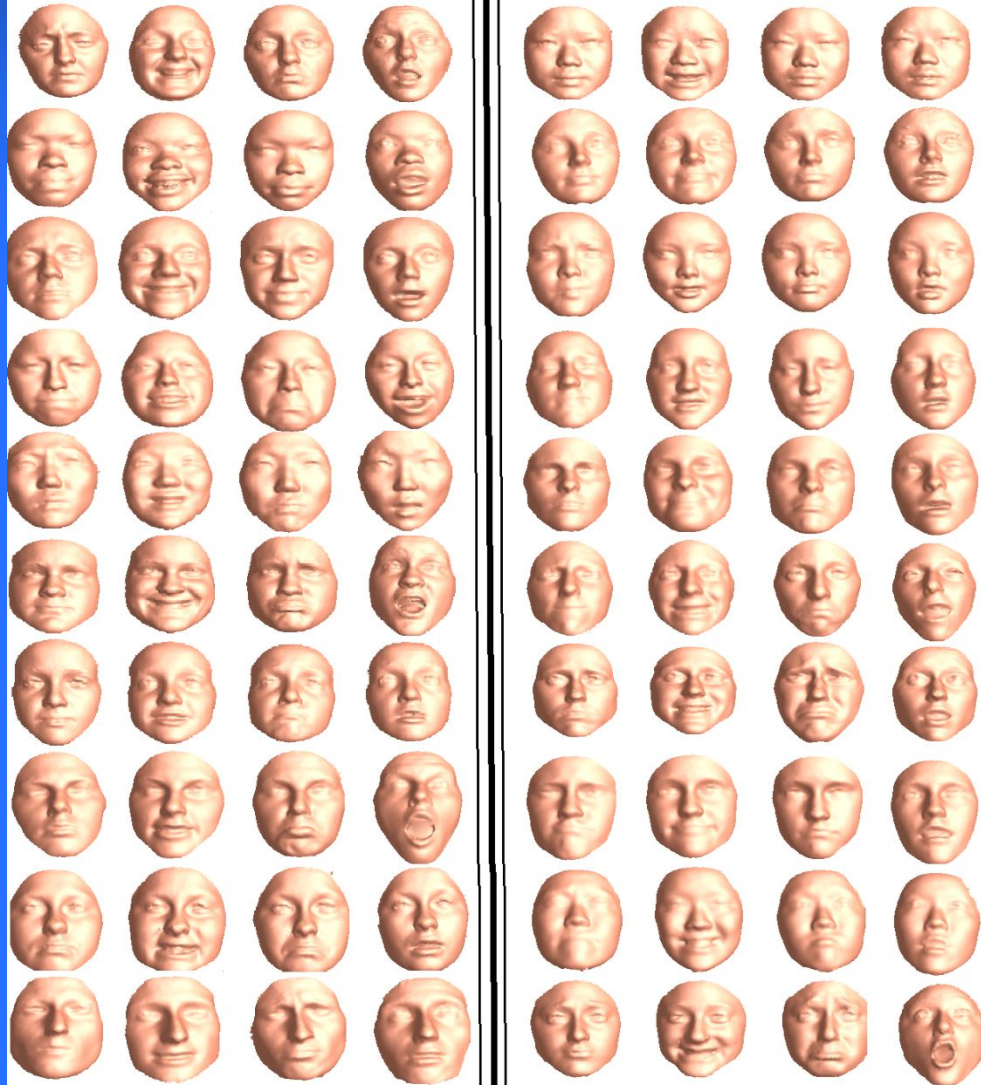
- Facial expression classification.



- Purpose:
  - Classify 3D human faces with different facial expressions.

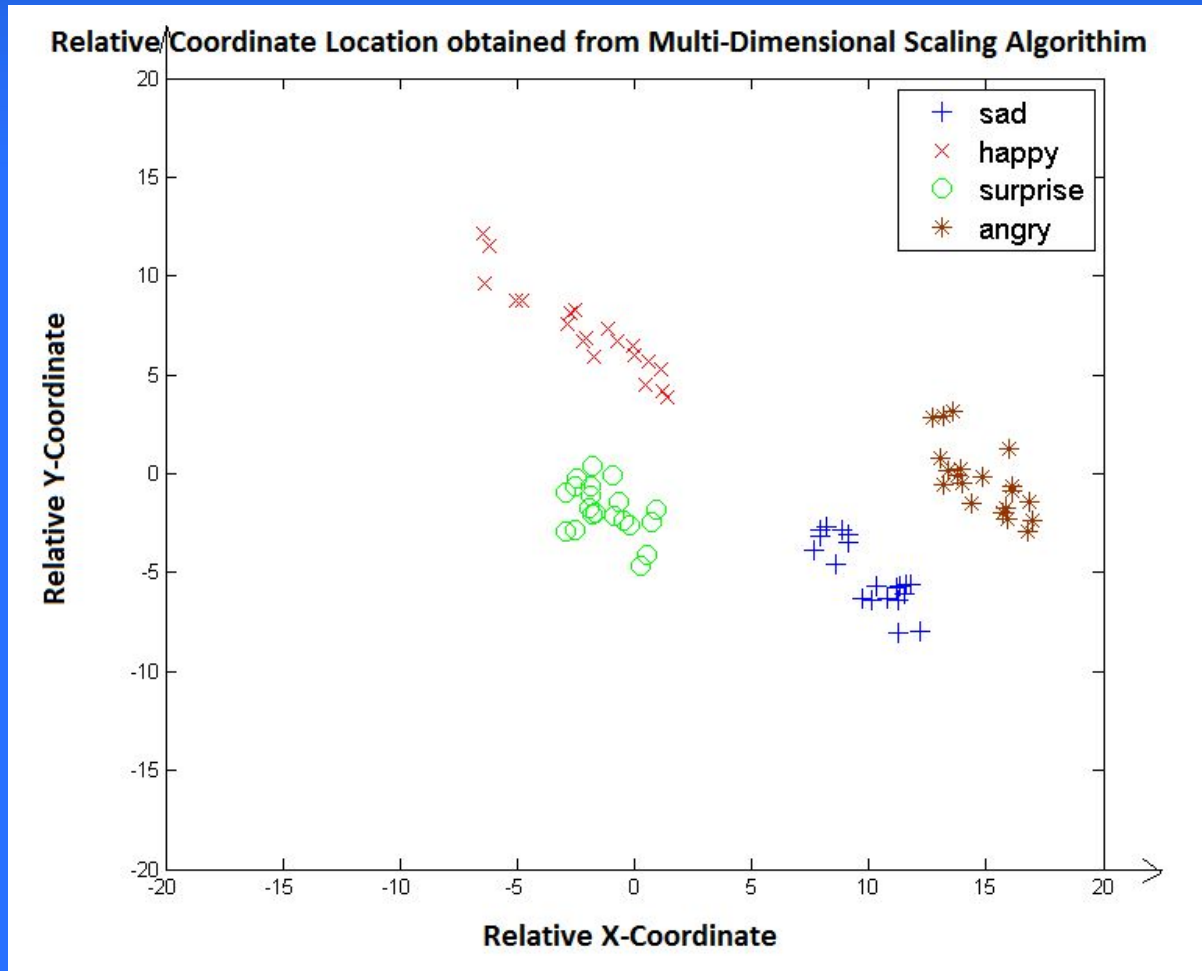
# Experimental results

- Dataset: 20 Angry + 20 Happy + 20 Sad + 20 Surprised



# Experimental results

- Visualization of the Wasserstein distance using a Multi-Dimensional Scaling (MDS) Algorithm



# Experimental results

- Brain classification with different IQ
  - Dataset: 50 males and 50 females, with ages ranging from 18 to 30 years old.
  - The intelligence quotient (IQ) was evaluated by an online version of Ravens Advanced Progressive Matrices, normalized ranging from 0-100, which are almost uniformly distributed.

# Experimental results

- Brain classification with different IQ
  - Settings: Instead of claiming whether one human brain is intelligent or not, in our experimental settings we divided the IQ into three classes: A, B, and C, ranging from A: [1,33], B: [34,67] and C: [68,100].
  - For each gender, we randomly chose 12 examples from each class as training set.

# Experimental results

Class A: 1,2,...,33

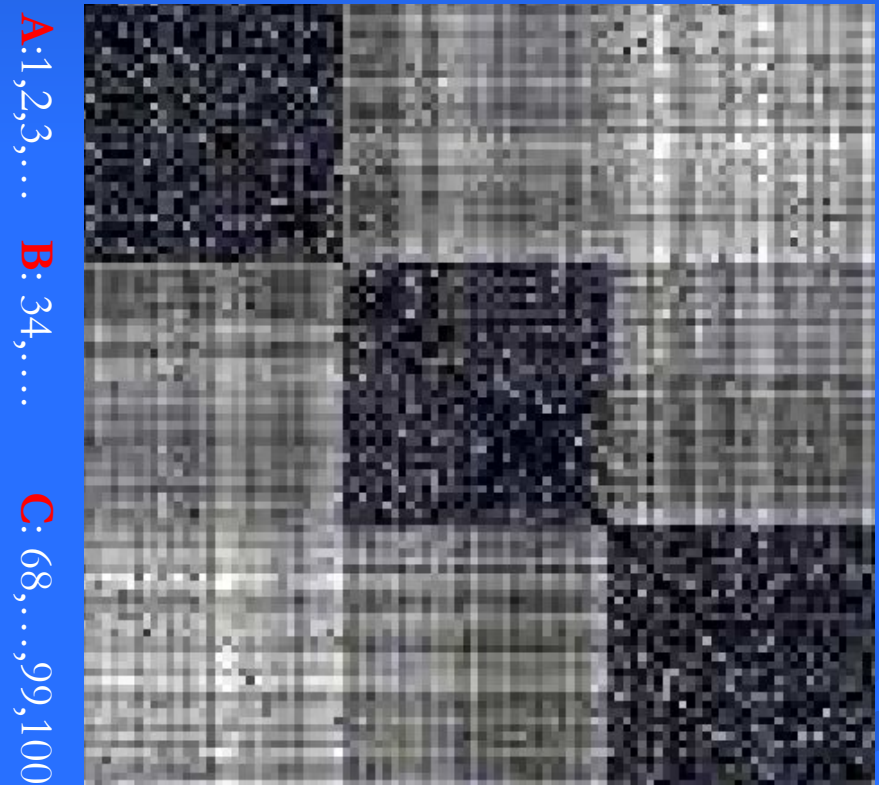
Class B: 34,35,...,67

Class C: 68,69,...,100

Entry(i, j) = WassDist(Brain i, Brain j).

**A**:1,2,3,...    **B**: 34,....

**C**: 68, ...,99,100



Wasserstein distance matrix grey image

# Experimental results

- With the distance matrix, we classified the testing set by k-Nearest Neighbors (k-NN) classifier.
- k is chosen to be 11 by running 9-fold cross-validation.

# Experimental results

- Comparison with other methods:

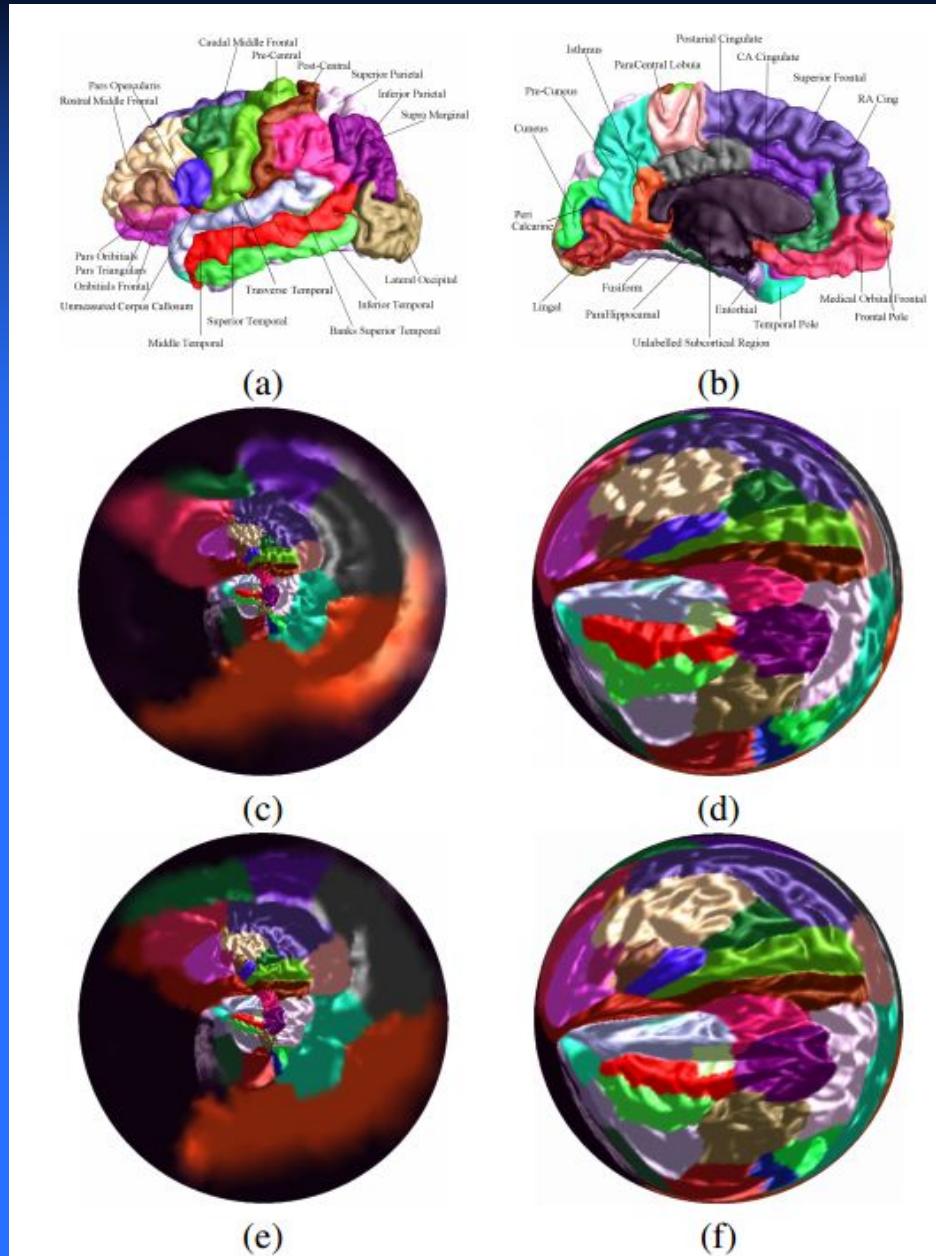
Method	CR
Our method	78.57%
Surface Area	53.57%
Surface Mean Curvature	57.14%
Combination of Area and Curvature	67.85%

Table 2. Classification rate (CR) of our method and previous methods based on cortical surface area, cortical surface mean curvature and combination of previous two cortical measurements. The results demonstrated the accuracy of our method.

- Related publications:
- Zhengyu Su, Yalin Wang, Rui Shi, Wei Zeng, Jian Sun, Feng Luo, Xianfeng Gu: Optimal Mass Transport for Shape Matching and Comparison. IEEE Transactions on Pattern Analysis and Machine Intelligence (T-PAMI), accepted on February, 2015.
- Zhengyu Su, Wei Zeng, Yalin Wang, Zhonglin Lu, Xianfeng Gu: Shape Classification using Wasserstein Distance for Brain Morphometry Analysis. Information Processing in Medical Imaging (IPMI), accepted on February, 2015.

# Area Preserving Brain Mapping

- Brain mapping transforms the brain cortical surface to canonical planar domains, which plays a fundamental role in morphological study.
- Most existing brain mapping methods are based on angle preserving maps.



# Application of Alzheimer's Disease Diagnosis

- Motivation:
  - For Alzheimer's disease (AD), structural MRI measurements of brain shrinkage are one of the best established biomarkers of AD progression and pathology.
  - The atrophy may not only be area shrinkage, but also have anisotropic directions.
  - Therefore, a good shape signature contains both area and anisotropic deformation information may have a good potential to be a practical biomarker.

# Area Preserving Brain Mapping

## ■ Our method:

- Proposed a novel biological shape signature based on optimal mass transport map and Beltrami coefficients.
- This signature encodes both area deformation and anisotropic deformation.
- Intrinsic to Riemannian metric
- The computation is stable, efficient and simple.

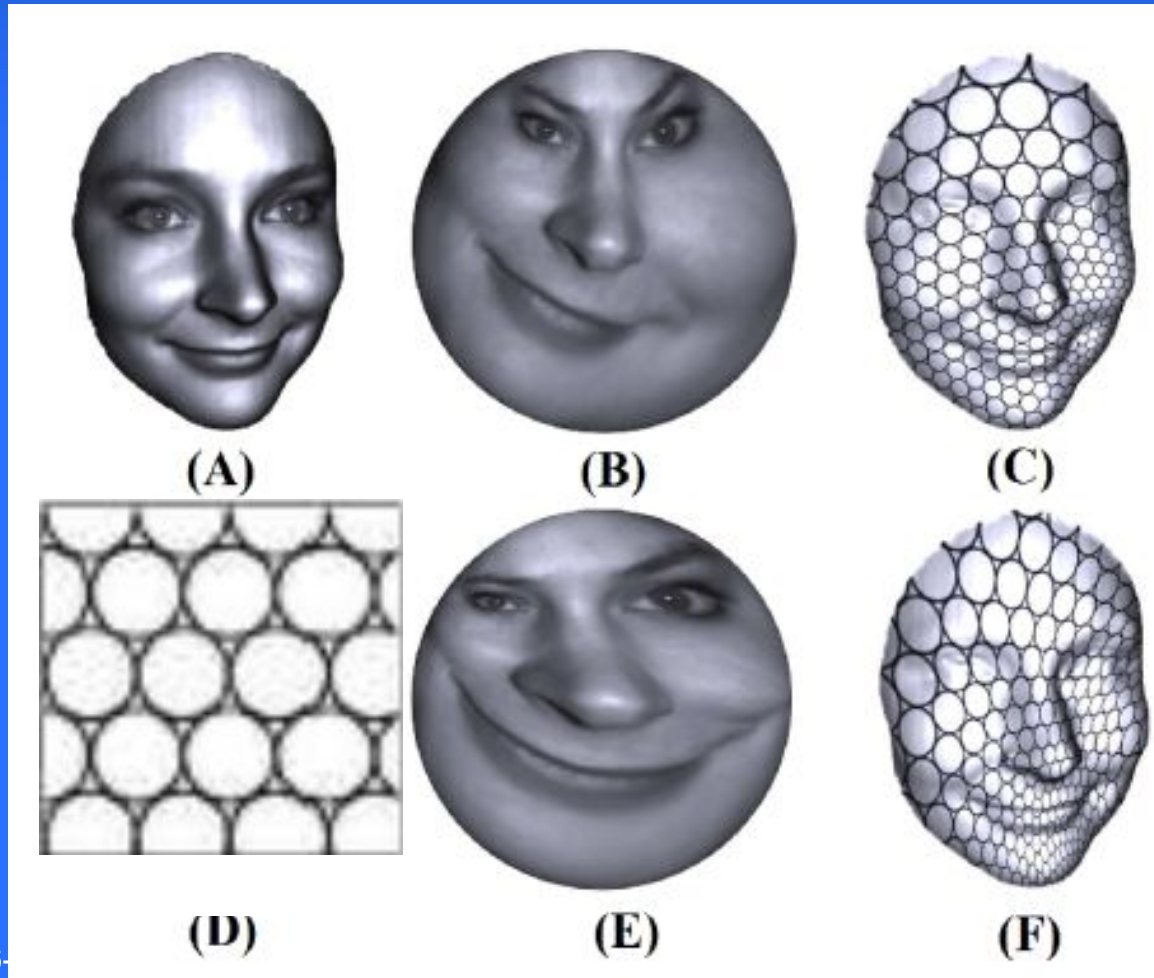
# Theoretic foundation

## ■ Beltrami coefficient:

- Defined on a local chart of any given surface, the Beltrami coefficient  $\mu$  is complex-valued and Lebesgue-measurable, satisfying  $|\mu| < 1$ , measures the distortion of a map.

# Theoretic foundation

## ■ Beltrami coefficients:



$|u| = 1$ , isotropic

$|u| < 1$ , anisotropic

# Algorithm

---

**Algorithm 2** Compute isometry invariant shape descriptors.

---

**Input:** Input brain cortical surface triangular meshes.

**Output:** Isometry invariant shape descriptors.

1. Cut along the cortical surface along surface curves and turn it into a genus zero surface with an open boundary.
  2. Compute its conformal mapping to the unit disk.
  3. Compute its Monge-Brénier based area-preserving mapping to the unit disk.
  4. Calculate the Beltrami coefficients between the conformal mapping result the area preserving mapping result and output them as isometry invariant shape descriptors.
-

# Application of Alzheimer's Disease Diagnosis

- We validated our method by using Beltrami coefficients as a shape signature to analyze the human brain cortical surfaces among AD patients and healthy (CTL) subjects.
- Dataset: 50 AD patients and 50 healthy control (CTL) subjects (Age: AD:  $75.86 \pm 7.65$ ; CTL:  $74.56 \pm 4.16$ ).

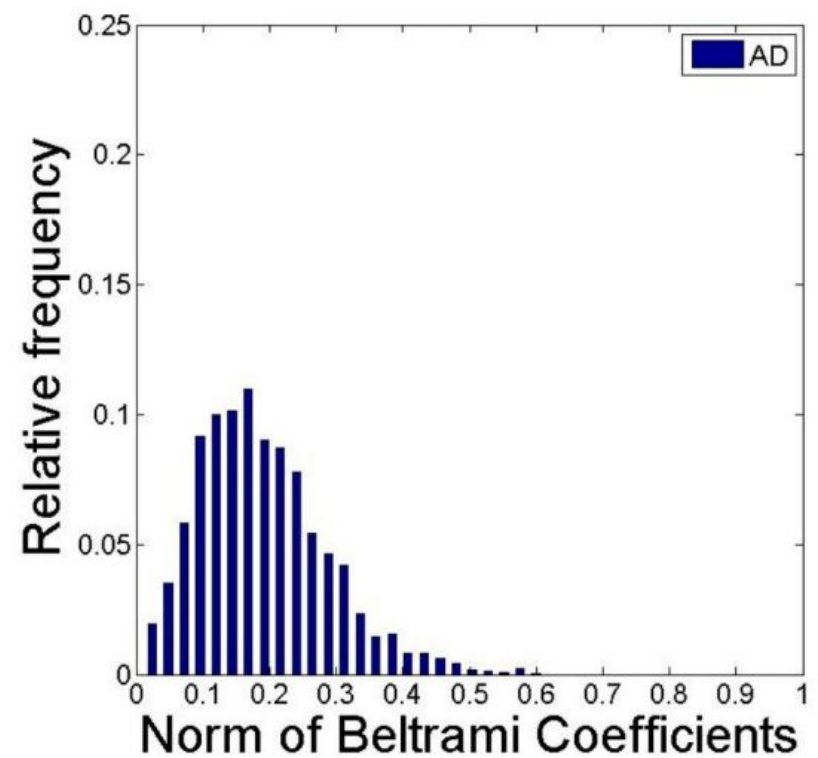
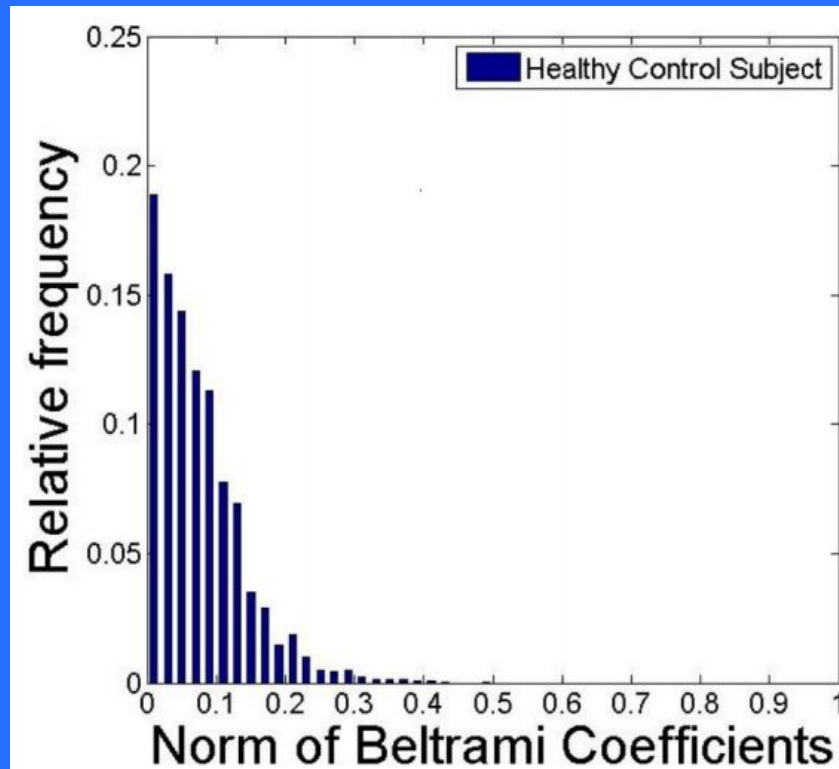
# Alzheimer's Disease Diagnosis

- We chose 3 functional areas to compute Beltrami coefficients. Middle Temporal, Superior Temporal and Fusiform, among the 10 most affected regions by AD according to previous work [1].

[1] Y. Shi, R. Lai, and A. Toga. Corporate: cortical reconstruction by pruning outliers with Reeb analysis and topology-preserving evolution. *Information Process Medical Imaging*, 22:233–244, 2011

# Application of Alzheimer's Disease Diagnosis

- The histograms show the norm of Beltrami coefficients of cortical surfaces of AD patients are obviously larger than those of healthy control subjects.



# Application of Alzheimer's Disease Diagnosis

## Classification settings:

- 80% data as training samples and the rest as testing samples.
- To obtain fair results, we randomly selected the training set each time and computed the average recognition rate over 1000 times.
- Support Vector Machine as a classifier, where the linear kernel function was employed, and we used C-SVM and chose  $C= 5$  by running cross validation.
- Compared with area based method and volume based method.

Method	Rate %
Area	70.00%
Volume	62.50%
Our method	87.50%

- Related publications:
- Zhengyu Su, Wei Zeng, Rui Shi, Yalin Wang, Jian Sun, Xianfeng Gu: Area Pre-serving Brain Mapping. IEEE Conference on Computer Vision and Pattern Recognition (CVPR), 2235 - 2242, Portland, Oregon, June, 2013.

# Optimal Mass Transport for Visualization

## ■ Motivation:

- With the fast generation of large and complicated data, it is desirable to develop new frameworks aiming at generating a visualization of the entire data for navigation, detection, and a global understanding of regions of interest (ROIs).

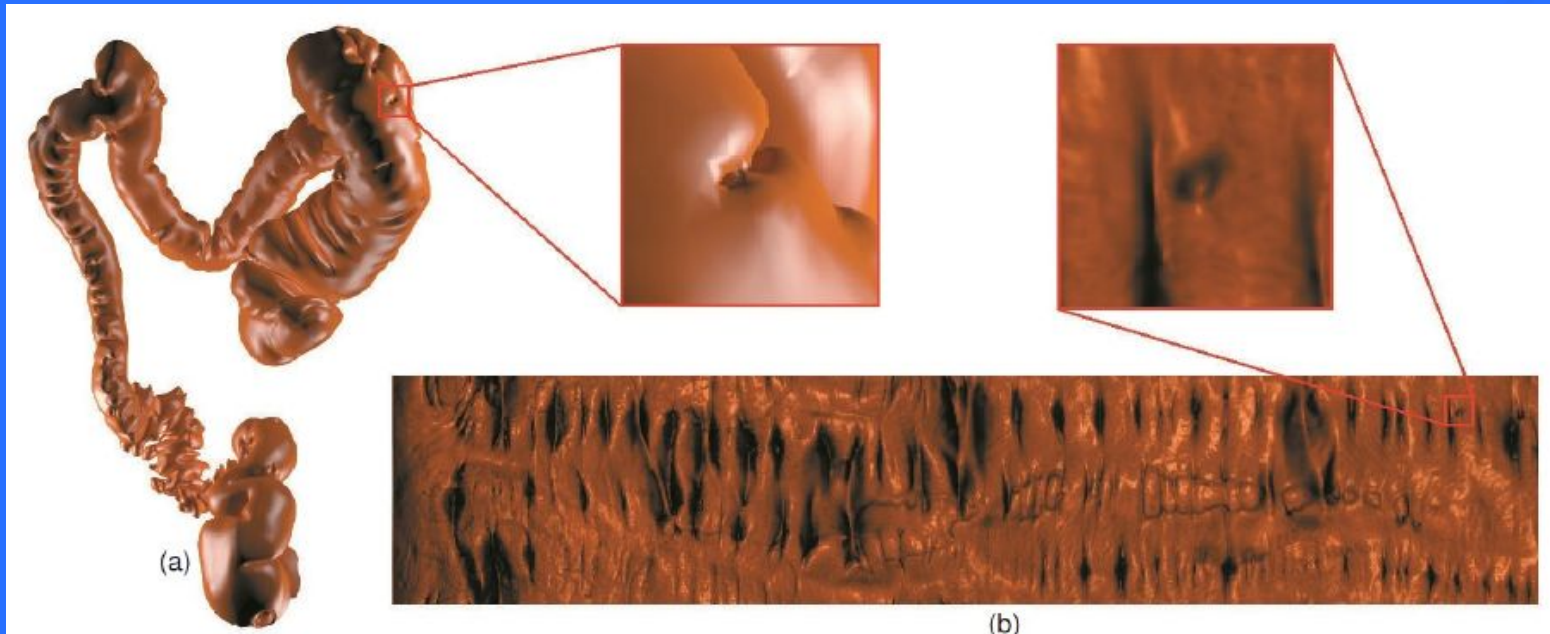
# Optimal Mass Transport for Visualization

## ■ Motivation:

- Surface flattening and texture mapping offer a good way of visualizing a surface section by enabling the visualization of all surface parts within a single planar image.
- In general, surface mapping will introduce distortions, either angle distortions or area distortions.

# Optimal Mass Transport for Visualization

- Existing conformal mapping method:
  - Conformal mapping offers a practical way of visualization that keeps local shape unchanged. This is important and useful for visual diagnosis.



# Optimal Mass Transport for Visualization

- Disadvantages of conformal mapping visualization
  - Substantially distorts area, which fails to display accurate size of area, including height, width, thickness or diameter of ROIs.
  - Unfortunately, these distorted area parameters are extremely important in many medical image recognition and auto diagnosis applications, studied in [1], [2]

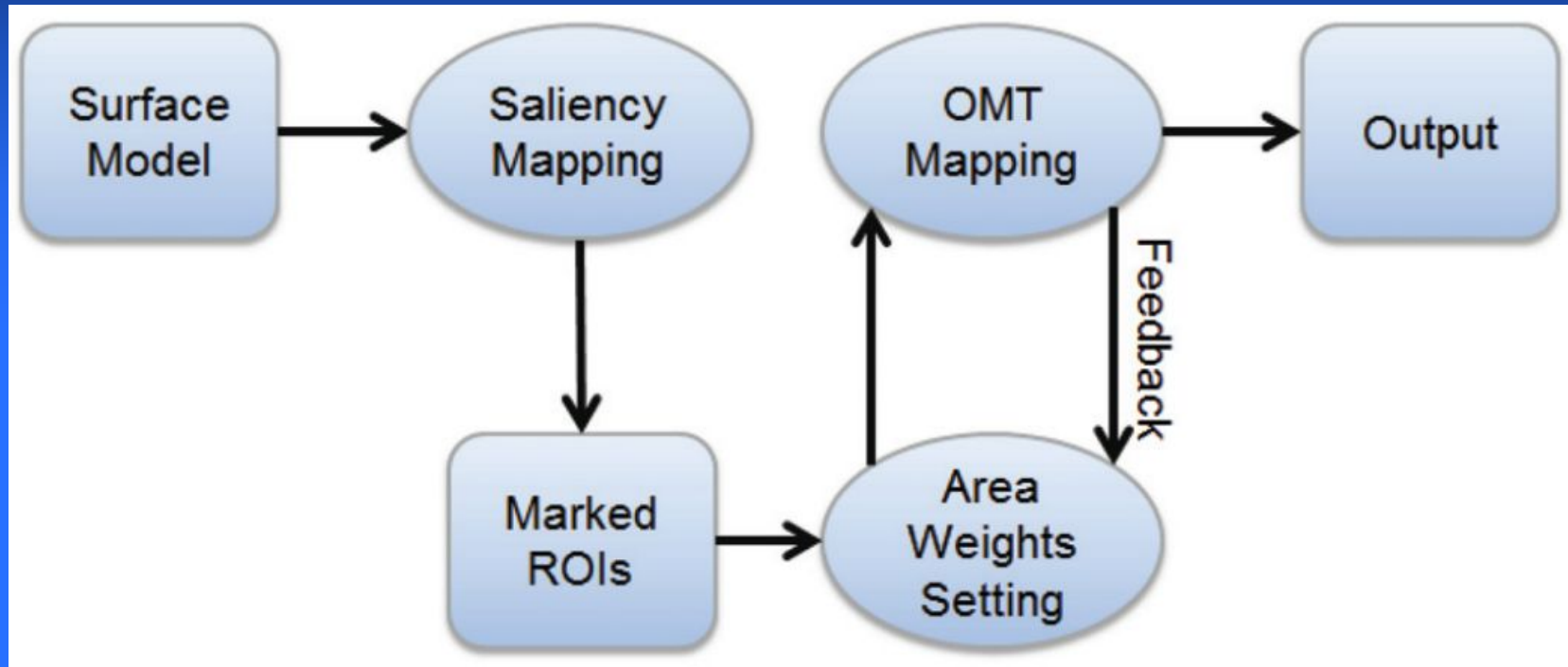
[1] S. Haker, S. Angenent, A . Tannenbaum , and R. Kikinis. Nondistorting flattening maps and the 3D visualization of colon CT images . IEEE TMI, 19(7):665–670, 2000.

[2] W. Zeng, J . Marino, A. E . Kaufman, and X . D . Gu. Volumetric colon wall unfolding using harmonic differentials . Computers and Graphics, 35(3):726—732, 2011.

# Optimal Mass Transport for Visualization

- An area-preserving mapping with flexible control of local information is highly desired.
- Our solution: Saliency visualization pipeline based on optimal mass transport map.

# Framework



# Importance driven visualization



(a) Front view



(b) Angle-preserving



(c) Area-preserving



(d) Back view



(e) 2x



(f) 3x



(g) 4x



(h) 6x

# Informatics visualization

## ■ Earth Map

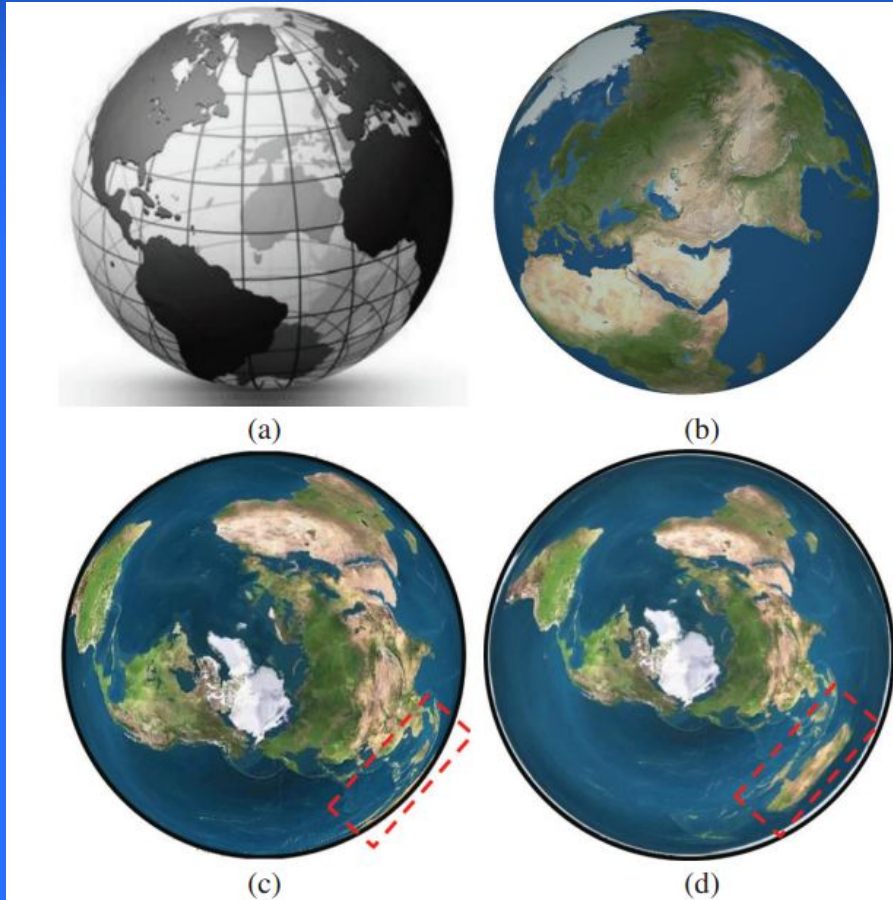


Fig. 7. Different mapping results and comparisons using an earth surface model. (a) A 3D earth model. (b) Direct projection mapping with large information loss. (c) Conformal mapping result with large area distortions. (d) Our area-preservation mapping result with accurate area preservation and small angle distortion (highlighted by the red frames).

## ■ Colon tumor detection

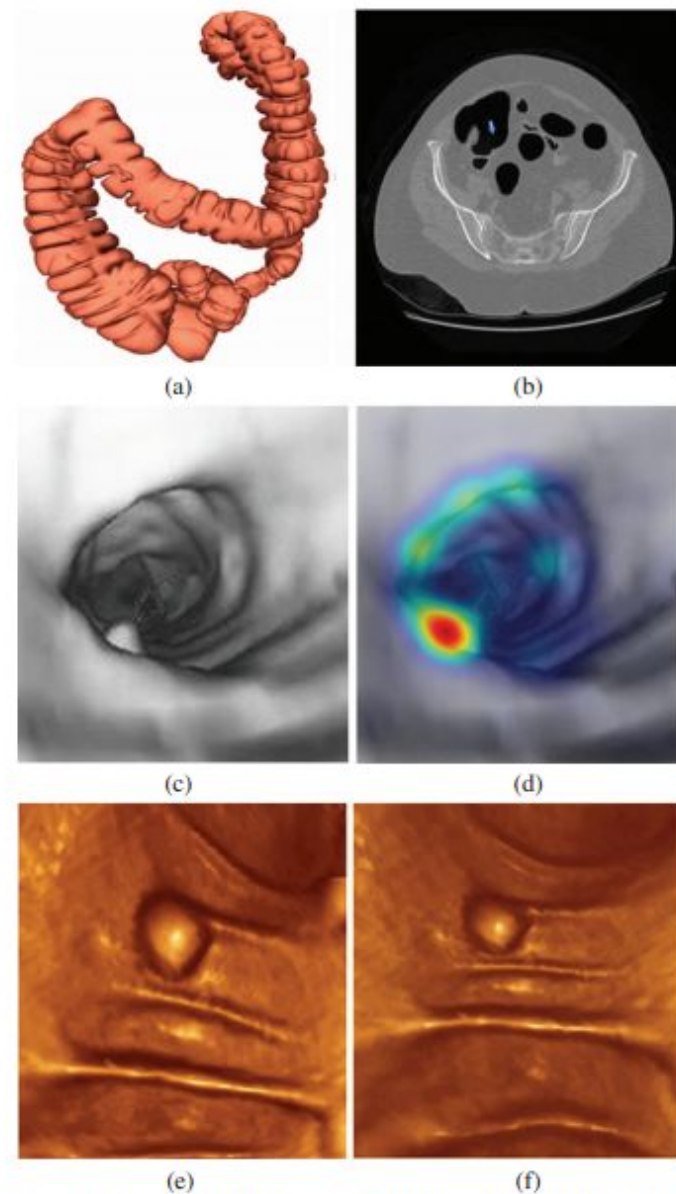


Fig. 6. Saliency map guided area-preservation mapping using a colon model. (a) A 3D colon surface, extracted from CT axis images, such as (b). (c) One possible polyp detected using (d) the saliency map [18]. Surface flattening results using (e) our area-preservation mapping and (f) conformal mapping. By comparison, our result generates the accurate polyp size for area measurement (verified by the doctor's measurement of the polyp as ground truth) without any severe angle distortion.

- Related publications:
- Xin Zhao, Zhengyu Su, Xianfeng Gu, Arie Kaufman: Area-Preservation Map-ping using Optimal Mass Transport. IEEE Transactions on Visualization and Computer graphics (TVCG), 19(12):2838-47, December, 2013

# Conclusion

- Introduced the optimal mass transport map algorithm based on Yau-Luo-Gu's variational principle, improves complexity from  $O(n^2)$  to  $O(n)$  in contrast to Kantorovich's approach.
- Applied in various research areas and applications, including computer vision, medical imaging and visualization.

# Future Directions

- Generalize the optimal mass transport map to from surface to volume, and even higher dimensions.
- Explore broader applications by optimal mass transport theory, such as wireless sensor network, machine learning, data science.

# Publications

- 4 Journal papers
- 5 Conference papers
- 1 Submitted

# Publications

- [1]. **Zhengyu Su**, Yalin Wang, Rui Shi, Wei Zeng, Jian Sun, Feng Luo, Xianfeng Gu: **Optimal Mass Transport for Shape Matching and Comparison.** *IEEE Transactions on Pattern Analysis and Machine Intelligence (T-PAMI)*, accepted on February, 2015.
- [2]. **Zhengyu Su**, Wei Zeng, Yalin Wang, Zhonglin Lu, Xianfeng Gu: **Shape Classification using Wasserstein Distance for Brain Morphometry Analysis.** *Information Processing in Medical Imaging (IPMI)*, accepted on February, 2015.
- [3]. **Zhengyu Su**, Wei Zeng, Rui Shi, Yalin Wang, Jian Sun, Xianfeng Gu: **Area Preserving Brain Mapping.** *IEEE Conference on Computer Vision and Pattern Recognition (CVPR)*, 2235 - 2242, Portland, Oregon, June, 2013.
- [4]. **Zhengyu Su**, Jian Sun, Xianfeng Gu, Feng Luo, Shing-Tung Yau: **Optimal mass transport for geometric modeling based on variational principles in convex geometry.** *Journal of Engineering With Computers*, 30(4):475-486, October, 2014.

# Publications

- [5]. Rui Shi, Wei Zeng, **Zhengyu Su**, Hanna Damasio, Zhonglin Lu, Yalin Wang, Shing-Tung Yau, Xianfeng Gu: **Hyperbolic Harmonic Mapping for Constrained Brain Surface Registration.** *IEEE Conference on Computer Vision and Pattern Recognition (CVPR oral)*, 2531 - 2538, Portland, Oregon, June, 2013.
- [6]. Xin Zhao, **Zhengyu Su**, Xianfeng Gu, Arie Kaufman: **Area-Preservation Mapping using Optimal Mass Transport.** *IEEE Transactions on Visualization and Computer graphics (TVCG)*, 19(12):2838-47, December, 2013.
- [7]. Wei Luo, **Zengyu Su**, Min Zhang, Wei Zeng, Junfei Dai, Xianfeng D. Gu: **Shape signature based on Ricci flow and optimal mass transportation.** *Journal of Optical Engineering*, April, 2014.
- [8]. Rui Shi, Wei Zeng, **Zhengyu Su**, Hanna Damasio, Zhonglin Lu, Yalin Wang, Shing-Tung Yau, Xianfeng Gu: **Hyperbolic harmonic brain surface registration with curvature-based landmark matching.** *Information Processing in Medical Imaging (IPMI)*, 23:159-70, 2013.
- [9]. Wei Zeng, Rui Shi, **Zhengyu Su**, David Xianfeng Gu: **Colon Surface Registration Using Ricci Flow.** *Abdomen and Thoracic Imaging*, 389-419, 2013.

# Submitted Paper

R. Shi, W. Zeng, Z.Y. Su, H. Damasio, Z.L Lu, Wang, Yalin, Yau, Shing-Tung; Gu, Xianfeng. Hyperbolic Harmonic Mapping for Surface Registration. Submitted to IEEE TPAMI

**Thank all the committee members:**

Professor. Xianfeng Gu

Professor. Jie Gao

Professor. Jing Chen

# Thanks !